Preparation and implementation of optofluidic neural probes for *in vivo* wireless pharmacology and optogenetics

Jordan G McCall[1–4], Raza Qazi[5], Gunchul Shin[6], Shuo Li[6,14], Muhammad Hamza Ikram[7], Kyung-In Jang[6,8], Yuhao Liu[6], Ream Al-Hasani[1–4], Michael R Bruchas[1–4,9,13], Jae-Woong Jeong[5,7,13] & John A Rogers[6,10–13]

[1]Department of Anesthesiology, Division of Basic Research, Washington University School of Medicine, St. Louis, Missouri, USA. [2]Washington University Pain Center, Washington University School of Medicine, St. Louis, Missouri, USA. [3]Department of Neuroscience, Washington University School of Medicine, St. Louis, Missouri, USA. [4]Division of Biology and Biomedical Sciences, Washington University School of Medicine, St. Louis, Missouri, USA. [5]Department of Electrical, Computer, and Energy Engineering, University of Colorado Boulder, Colorado, USA. [6]Department of Materials Science and Engineering, Frederick Seitz Materials Research Laboratory, University of Illinois at Urbana-Champaign, Urbana, Illinois, USA. [7]Materials Science and Engineering Program, University of Colorado Boulder, Colorado, USA. [8]Department of Robotics Engineering, Daegu Gyeongbuk Institute of Science and Technology (DGIST), Daegu, Korea. [9]Department of Biomedical Engineering, Washington University, St. Louis, Missouri, USA. [10]Department of Electrical and Computer Engineering, University of Illinois at Urbana-Champaign, Urbana, Illinois, USA. [11]Department of Mechanical Science and Engineering, University of Illinois at Urbana-Champaign, Urbana, Illinois, USA. [12]Department of Chemistry, University of Illinois at Urbana-Champaign, Urbana, Illinois, USA. [13]These authors contributed equally to this work. [14]Present address: Department of Materials Science and Engineering, Cornell University, New York, USA. Correspondence should be addressed to M.R.B. (bruchasm@wustl.edu), J.-W.J. (jaewoong.jeong@colorado.edu), or J.A.R. (jrogers@uiuc.edu).

Published online 5 January 2017; doi:10.1038/nprot.2016.155
This protocol is an extension to *Nat. Protoc.* **8**, 2413–2428 (2013); doi:10.1038/nprot.2013.158; published online 7 November 2013

This Protocol Extension describes the fabrication and technical procedures for implementing ultrathin, flexible optofluidic neural probe systems that provide targeted, wireless delivery of fluids and light into the brains of awake, freely behaving animals. As a Protocol Extension article, this article describes an adaptation of an existing Protocol that offers additional applications. This protocol serves as an extension of an existing Nature Protocol describing optoelectronic devices for studying intact neural systems. Here, we describe additional features of fabricating self-contained platforms that involve flexible microfluidic probes, pumping systems, microscale inorganic LEDs, wireless-control electronics, and power supplies. These small, flexible probes minimize tissue damage and inflammation, making long-term implantation possible. The capabilities include wireless pharmacological and optical intervention for dissecting neural circuitry during behavior. The fabrication can be completed in 1–2 weeks, and the devices can be used for 1–2 weeks of *in vivo* rodent experiments. To successfully carry out the protocol, researchers should have basic skill sets in photolithography and soft lithography, as well as experience with stereotaxic surgery and behavioral neuroscience practices. These fabrication processes and implementation protocols will increase access to wireless optofluidic neural probes for advanced *in vivo* pharmacology and optogenetics in freely moving rodents.

INTRODUCTION

An understanding of the complex circuitry of the mammalian brain remains one of the chief goals of modern neuroscience and holds promise for novel therapeutic interventions for many neurological and psychiatric disorders[1]. To help decode this complex circuitry, a number of genetic tools for selectively modulating molecularly defined neuronal subtypes have been developed by several groups[2–10]. In these efforts, it is important to note that two primary solutions have emerged: one using photons to target exogenously expressed channels, pumps, or receptors, or to alter gene expression (optogenetics)[11–16], and one using highly selective ligands to target exogenously expressed channels and receptors (chemogenetics)[17]. Perhaps the most powerful application of these tools is in awake, behaving animals in which fundamental insights into neural function are emerging at an extraordinary rate[18]. Either genetic tool set requires external hardware to deliver the targeting agents. For optogenetics, this hardware most frequently takes the form of implantable fiber optics coupled to an external light source[16], although more recent advanced approaches have offered a more spatially selective light delivery[19–24]. For chemogenetics, the typical route of administration is a systemic (commonly intraperitoneal) ligand injection. In some instances, however, neural circuit dissection with chemogenetics is aided by local delivery within the brain[25]. In either case, the study of more naturalistic behaviors can benefit from a wireless approach that allows the untethered behavior of the investigated animal.

Many approaches to wireless optogenetics have been demonstrated by our group and others[21,22,26–34], but these devices lack an interface for delivery of fluids such as viral vectors, therapeutic drugs, or other pharmacological agents. Here we describe the fabrication and implementation of new devices that maintain the ability to wirelessly photostimulate but now offer additional capabilities in wirelessly programmable fluid delivery. This Protocol Extension article builds on our earlier protocol by McCall *et al.*[35], which described procedures for fabricating flexible, wireless ultrahigh-radiofrequency-powered optoelectronic devices for optogenetic applications and for measuring electrophysiological, thermal, and photonic properties of brain tissue. Although the devices detailed in our earlier protocol[35] enable unique experimental utility for wireless photostimulation, they are limited in scope in regard to other wireless perturbations such as localized pharmacological manipulations within deep brain structures. Local region-selective pharmacology is a robust tool that is widely used in dissecting both neural circuits and endogenous receptor/ligand systems. To date, however, localized fluid infusion has relied exclusively on tethered cannula-based methods. We recently reported a system that is capable of wireless fluid delivery that can be combined with optogenetics in

a single platform[36]. These optofluidic neural probes can deliver up to four different fluids, with demonstrated functionality in viral gene transfer, small-molecule or peptide pharmacology, and simultaneous optogenetic pharmacological manipulations. Importantly, these probes do not require external connection to independently located light and fluid sources, allowing free movement of the research subject and reduced equipment requirements for the experimenter. The combined functionality of these probes is optimized to directly manipulate the same local circuitry and neurotransmitter systems in a spatially precise manner. If an experiment requires separately manipulated brain structures (i.e., photostimulation in one region and pharmacological manipulation elsewhere), then combinations of traditional tethered approaches may be more feasible. For those adopting this protocol, these optofluidic neural probes will serve as a unique and versatile tool for further dissection of neural circuitry.

Development of the protocol

This protocol began as an extension of our previous work[21,35], although the final design represents a distinct platform with features that are entirely independent of previous devices and applications. Although our earlier protocol described devices that provide multimodal access to the CNS, these devices lacked the ability to deliver fluids into the brain[21,35]. To achieve wireless fluid delivery, we critically examined available fluid delivery strategies (i.e., cannulation[37,38], reverse microdialysis[39], iontophoresis[40,41]) and ultimately decided to follow a strategy that most closely mimics the pump/infusion model of a traditional cannula approach. We identified a strategy to render these systems into head-mountable formats for intracerebroventricular drug delivery[42] and sought to reduce the physical dimensions to allow brain-site-specific delivery and enable wireless control. The simplified approach involves a system based on soft, elastomeric microfluidic channels, an active pumping system, and thin, flexible control electronics. The resulting platform is suitably lightweight and well tolerated by mammals as small as mice.

Alternative methods

Comparison with other wireless fluid delivery devices. Traditional methods for intracerebral fluid delivery involve implantation of a metal tube/cannula that is connected to an external tubing system and infusion pump. Although this technology is easily accessible and can now be paired with multifunctional fibers for photostimulation[43], it is not readily available for wireless adaptation. Similarly, systems that enable wireless drug delivery are not sufficiently small/lightweight to be tolerated in small mammals such as mice, nor are their delivery quanta on the proper scale for intracerebral manipulations[44–47]. An exception to the latter limitation was demonstrated in a recently reported system referred to as 'e-dura'[48]. However, this approach required tethered operation to allow drug delivery[48]. The current protocol overcomes constraints of both wireless delivery and scale to enable access to common rodent animal models. However, it is important to note that previously reported tethered devices, such as multifunctional fibers[43] and e-dura[48], offer capabilities in electrical recording and/or stimulation that our current protocol lacks. Furthermore, the current protocol details devices that are optimized for combined pharmacological and optogenetic manipulations in a localized manner at the same brain site.

Comparison with other devices for wireless optogenetics. To meet the power demands of the microfluidic system and to ensure consistent operation at programmed time points, this protocol adopts a battery-powered approach rather than the radiofrequency (RF) power harvesting approach of the previous protocol[35]. The advantage of using a battery-powered microprocessor is that it allows for greater current delivery and avoids potential orientation and polarization issues associated with RF power harvesting[21,26–28,35]. One implication of this change is that the pulsing paradigms must be pre-programmed into the control electronics. In other words, one must select a set of experimental parameters before preparation of the wireless modules. This protocol describes four different pulse frequencies. External modification of these pulse parameters is possible, but those reported here provide a base framework (i.e., it is possible to convert a free-running 20 Hz paradigm to a discrete, triggered burst at 20 Hz, but it is not possible to change the pulse width externally). For wireless control, we use IR approaches because they are compatible with most environments as reflections of the IR light enable use even in the absence of a direct line of sight.

Applications of the method

This protocol and our previous publication[36] focus exclusively on implementation of these devices for neural circuit dissection using viral, pharmacological, and optogenetic approaches in the rodent brain. It is reasonable to assume that small alterations of this protocol would enable access to the spinal cord and possibly the peripheral nervous system as well; however, these approaches have not yet been explored. Local delivery of drugs in such cases could provide opportunities for better pain management and/or aid in regeneration of damaged nerves[48–50]. Similarly, minor adaptations could also enable optical pharmacology approaches, to 'uncage' or 'photo-switch' various molecules. Integration of the optofluidic neural probes with microscale inorganic light-emitting diodes (μ-ILEDs) that emit UV light would expand the applicability of these devices to wild-type animals and increase the chance of therapeutic translation using caged compounds[51–54]. This protocol also suggests approaches for providing external or closed-loop wireless control of the device hardware. To this end, these platforms enable pre-programmed or semiautomatic experimentation. Granting external control to the IR remote (e.g., to an input/output (I/O) box or timer) allows the researcher to plan fluid delivery or photostimulation to happen at a later time point, in the home cage, or in response to the animal's behavior. The need for, and implications of, such an approach will vary widely across laboratories, but it is important to note that such methods are immediately feasible with the protocol described here.

Limitations

The wireless schemes used by these probes are entirely distinct from those presented in the previous protocol[35]. Although these battery-powered designs are larger (~1.8 g) than the current generation of RF harvesters[22,26–28,34], size reduction for devices intended exclusively for photostimulation is immediately possible. The power requirements for the μ-ILED are substantially less than those of the Joule heaters needed for fluid delivery. Furthermore, control of the pulse paradigm for photostimulation could be removed from the onboard microcontroller and instead be handled remotely by pulsing the IR signal. In other

words, the system could be constructed such that an IR sensor directly modulates the μ-ILEDs based on incoming IR signals. In this way, the IR signal could be pulsed to any desired parameters. Such modifications could likely enable a wireless photostimulation device that weighs less than 500 mg, without the orientation limitations that constrain RF-based approaches[21,26–28,35].

Unlike the previous protocol[35], the optofluidic neural probes presented here are mostly fabricated from readily available and/or 3D-printable materials in a standard lab environment. However, utility of these devices may be limited by how the fluid chambers are filled (Steps 28–32). The current design allows each set of four chambers to be filled once. Development of a cartridge system that can reversibly connect to the microfluidic channels is one possibility for overcoming this hurdle. In this case, disposable cartridges could be filled with fluid, and once the fluid is dispensed from all chambers in the cartridge, the entire cartridge could be replaced. Similarly, these devices are not necessarily intended for chronic, long-term application. Although the optoelectronic features of the device should function for at least 6 months[21,35], the fluid chambers are not designed for fluid storage beyond 1–2 weeks. This issue can probably be overcome with further encapsulation of the fluidic components, but such an approach would add some weight to the device and has yet to be directly tested. Importantly, the functional lifetime of the optoelectronic components is dependent on battery power; therefore, chronic (>2 weeks) optical stimulation requires a surgical approach, which involves implantation of only the probe hardware to be paired acutely with the powering unit at the time of the experiment.

Experimental design

Fluid delivery. The optofluidic neural probes presented here have been used to deliver a variety of different fluids, including adeno-associated viruses, synthetic neuropeptides, and small-molecule antagonists[36], without any notable degradation in the efficacy of these substances *in vivo*. We have recently validated these conclusions in multiple behavioral and anatomical assays[36]. Not all fluids, however, will be immediately compatible with this delivery system. In particular, the thermal stability of the fluid should always be considered. Although we have used these devices to successfully deliver adeno-associated virus (serotype 5; AAV5; ref. 36), we have not tested other commonly used viruses. Many of these viral targeting methods (e.g., adenovirus[55], lentivirus[56,57], rabies[58], herpes simplex[59], and canine adenovirus[60]) have different thermal stabilities than those of AAV5 (ref. 61) that may present issues associated with long-term storage at room temperature (23–25 °C) and the transient heating applied by the devices. Once the fluidic chambers are implanted above the animal's skull, those fluids will remain exposed to light and at room temperature until the experimenter chooses to begin the infusion. In addition, the infusion itself briefly raises the temperature of the fluid to ~55 °C (depending on the specific heat of the fluid), but it rapidly cools to physiological temperature along the microfluidic channel before entry into the brain. According to our experimental and computational analysis, the temperature of fluid at the exit port of the microfluidic probe is <0.1 °C higher than the physiological temperature (~37 °C; ref. 36). Importantly, thermal inactivation of viruses depends on both the temperature and duration of heating; we therefore expect limited inactivation based on the transient nature of the temperature increase (~5 s at ~55 °C). Given these inherent temperature changes, it is critical that the thermal and optical stability of desired fluids be tested before *in vivo* administration.

Subjects. This protocol and these devices have been optimized for use in adult rodents. To date, these probes have been used with adult (25–35 g) male and female C57BL/6J mice, mutant mice back-crossed to the C57BL/6J mouse strain, and adult (275–325 g) male Lewis rats. These devices are readily adaptable for use in other mammalian animal models. When considering application in a new model organism, care should be taken that the probe depth and volume of fluid delivery are appropriate. The designs presented here can access the cortex of most mammalian animal models, but the dimensions may need to be adjusted for deep brain structures in larger animals. The delivered volume and probe length share some co-dependency. The appropriate size of the fluid chamber for a longer microfluidic probe should be empirically determined before use *in vivo*. In addition, it is noteworthy that we have found that multiple C57BL/6J mice with implanted optofluidic probes can cohabitate without damage to the systems. Animals with a high degree of mutual exploration and curiosity may, however, be able to damage these devices. In such cases, cohabitation with dummy devices should be attempted before beginning an experiment. Before beginning this protocol, all the procedures described herein should be approved by the animal care and use committee of the investigating institution and conform to national guidelines and regulations regarding animal research. For this protocol, all procedures were approved by the Animal Care and Use Committee of Washington University in St. Louis and conformed to US National Institutes of Health guidelines.

Surgery. Although the basic surgical approach is similar to that of any stereotaxic surgery[16,35,40,41,62–65], and the theory is the same as that of our previous protocol[21,35], it is important to recognize certain unique aspects related to implanting optofluidic neural probes. We previously reported two feasible approaches to implantation: chronic implantation of the fully self-contained optofluidic device (approach 1) and implantation of only the probe hardware to be paired acutely with the powering unit at the time of the experiment (approach 2)[36]. The choice between these two options rests largely on the specific circumstances of the researcher. First and foremost, the animal model should be considered. Although we were unable to detect meaningful negative impact on the behavior of C57BL/6J mice with chronically implanted full systems (approach 1), it is clear that larger animals, such as rats, will tolerate the self-contained system better than smaller animals such as mice. However, there are many other factors worth considering before surgery. For example, if resources are limited and animal experiments are performed individually, then approach 2 is likely a better option, as it allows unlimited numbers of study subjects using a single set of wireless control electronics and batteries. Depending on accessibility to the stereolithography system described here, some groups may opt to fabricate a discrete set of device cases for use in repeated experiments. However, if the aim of the study is to achieve preprogrammed behavioral studies, then approach 1 is clearly advantageous, as the experimenter never needs to physically engage with the animal for experimental manipulations following the surgery.

Another point of consideration arises from the experimental or procedural need for a completely flexible probe. In other words, the successful removal of the stainless steel microneedle is one of the more challenging aspects of the surgery, and it is not always completely necessary. A variation on the described surgery does not include the removal of the microneedle. This approach is still well tolerated, as the microneedle described here is an order of magnitude smaller than those used in previously described systems[21,35,36]. Removal of the microneedle is best done on a two-armed stereotax (e.g., KOPF Model 942), as described here. However, we have performed the surgery on single-arm stereotaxes (KOPF Models 940 and 1900) and used forceps to manually remove the microneedle as well. This latter approach is feasible, but it requires a well-practiced surgeon. Furthermore, a bespoke stereotaxic adaptor could be commissioned for these surgeries, but we have found the described procedures to provide accurate and safe implantation.

One final consideration applies to experiments involving viral manipulations. These devices are capable of delivering viruses themselves. As a result, prior surgery to inject virus or a viral injection step before implantation in the same surgery may not be necessary. In other words, one may choose to implant a device that has one (or more) chamber loaded with the virus of choice (e.g., for the expression of an optogenetic or chemogenetic construct) so that the device can deliver the gene of interest and then later pharmacologically or optically probe the same tissue. This approach limits the number of subsequent pharmacological interventions from the device (i.e., a four-chambered device can deliver only three other compounds if one chamber is used to deliver virus). Furthermore, it is important to weigh the time line of the experiment with the lifetime of the device. The onboard battery life is greatly affected by the chosen operations of the device (i.e., amount of photostimulation and/or number of heaters engaged), and it will also decay below operational use in 1–2 weeks. More specifically, the device consumes 1.39 milliampere hours (mAh) for each LED blink with a 10-ms pulse width and 0.24 mAh for each heater operation for 20 s. We strongly urge those adopting this protocol to empirically determine the battery consumption of the chosen experimental paradigm before making surgical decisions. Regardless of the surgical approach adopted, it is critical that the researcher keep the well-being of the study subject and the experimental end point in mind as decisions are made. It is likewise imperative that all procedures be approved by the local animal care and use committee and conform to national guidelines and regulations.

Controls. Our previous protocol noted the importance of the proper controls for optogenetics[11,16,21,35], and these same considerations still apply. However, one notable advantage of these devices is their inherent suitability for within-subject design[36]. The experimental power of such an approach should be carefully weighed against the practical considerations of drug clearance (i.e., are multiple pharmacological treatments feasible given the properties of the agents used?), behaviors being assessed (i.e., does novelty of exposure to an assay play a crucial role in the observed behavior?), and whether a truly counterbalanced design is possible. It is also critically important to note that within-subject designs involving photostimulation vs. no photostimulation do not obviate the need for expressing opsin-negative, fluorescent-reporter-only controls.

MATERIALS

REAGENTS

Preparation of microfluidic probes

- Pt inhibitor [3-(2-aminoethylamino)propyl]trimethoxysilane (AEAPS; Sigma-Aldrich, cat. no. 440302)
- Chlorotrimethylsilane (TMCS; Sigma-Aldrich, cat. no. 386529) **! CAUTION** TMCS is toxic and flammable. Wear gloves and a mask, and use eye protection when using TMCS.
- Methanol (Fisher Scientific, cat. no. A411) **! CAUTION** Methanol is flammable.
- Acetone (Fisher Scientific, cat. no. A18) **! CAUTION** Acetone is flammable.
- Isopropyl alcohol (IPA; Fisher Scientific, cat. no. A415) **! CAUTION** IPA is flammable.
- Polydimethylsiloxane (PDMS; Dow Corning, cat. no. Sylgard 184)
- UV-curable epoxy (SU-8 10, MicroChem, cat. no. Y131259 0500L 1GL)
- SU-8 developer (MicroChem, cat. no. Y020100 4000L 1PE)
- Polycarbonate sheets (PC; McMaster-CARR, cat. no. 85585K103)

Preparation of thermally actuated pumps

- Parylene C (dichloro-di-para-xylylene (DPX-C); Specialty Coating Systems)
- Thermally expandable microspheres (Expancel microspheres; AkzoNobel, cat. no. 031 DU 40)
- PDMS (Dow Corning, Sylgard 184)
- Cyclic olefin polymer (COP; Zeonor, cat. no. 1420R)
- FR4 sheets (G10 glass epoxy sheets; ePlastics, cat. no. G10NAT0.016X12X12)
- Ultrathin double-faced polyester film (Adhesive Research, cat. no. ARclear 8154)
- Positive photoresist (Clarivant, cat. no. AZ5214E)
- AZ 917MIF developer (Integrated Micro Materials, cat. no. AZ 917MIF)
- Chrome (Cr) etchant (HTA Enterprises, cat. no. CEP-200)
- Gold (Au) etchant (Transene, cat. no. TFA)
- Silver epoxy (MG Chemicals, cat. no. 8331)
- 5 Minute Epoxy (Devcon, cat. no. 14250)

Preparation of μ-ILED probes

- Reagents required to prepare μ-ILED probes are described in our previous protocol[35]

Preparation of releasable injection needles

- Tungsten sheet (50-μm-thick, Goodfellow Group, cat. no. W000240)
- Silk adhesive (provided by Tufts university; Details are shown in other papers[66–68])

Implantation of optofluidic probes into the target brain region

- Adult (25–35 g) male or female C57BL/6J mice (Charles River, cat. no. 027), mutant mice (Jackson Laboratory, cat. no. 008601) back-crossed to the C57BL/6J mouse strain, and adult (275–325 g) male Lewis rats (Charles River, cat. no. 004) **! CAUTION** Before beginning this protocol, the animal care and use committee of the investigating institution should approve all procedures, which should conform to national guidelines and regulations regarding animal research.
- Isoflurane, US Pharmacopoeia (USP; Isothesia; Butler Schein, cat. no. 029405) or another approved anesthetic agent **! CAUTION** Ensure that proper ventilation and gas scavenging methods are in place to prevent potential inhalation of excess isolflurane.
- Betadine solution (Purdue Products, cat. no. 67618015017)
- Ethanol (Sigma-Aldrich, cat. no. 362808) **! CAUTION** Ethanol is flammable.
- Hydrogen peroxide, 3% (wt/vol), USP (Select Medical Products, cat. no. 117)
- Lidocaine ointment, USP, 5% (wt/wt) (Fougera)
- Ophthalmic ointment (Altalube Ophthalmic Product)
- Dental cement (Jet Denture Repair; Lang Dental, cat. no.1223; see Reagent Setup) **! CAUTION** Methyl methacrylate monomer, stabilized, is a flammable liquid. It may also cause skin irritation; avoid contact with skin, eyes, and clothing. Use with adequate ventilation.
- 0.9% (wt/vol) Sodium chloride Injection, USP (9 mg/ml NaCl; Hospira, cat. no. RL-0497(9/04))

- Enroflaxin (Baytril, Bayer, cat. no. R30901)
- Antibiotic ointment (Neosporin; Johnson & Johnson, cat. no. 174-73087Q)
- Artificial cerebral spinal fluid (ACSF; Tocris, cat. no. 3525, or custom, see Reagent Setup[14,69])

Fluids for wireless delivery

- Pharmacological agents: we previously used [D-Ala^2, NMe-Phe^4, Gly-ol^5]-enkephalin (Tocris, cat. no. 1171) and SCH 23390 hydrochloride (Tocris, cat. no. 0925) dissolved in ACSF; see Reagent Setup ▲ **CRITICAL** Not all pharmacological agents will be compatible with delivery from these devices. If the agent in question cannot be maintained in a well-lit room at room temperature, or is sensitive to transient heating (~5 s at ~55 °C), it may not be compatible with these devices. *In vitro* testing of such agents under conditions similar to those of injection is advised.
- Viruses: we have used adeno-associated viruses from the WUSTL Hope Center Viral Core (https://hopecenter.wustl.edu/?page_id=99) and the University of North Carolina Viral Vector Core (http://genetherapy.unc.edu/services.htm). Lentiviruses are also available from the WUSTL Hope Center Viral Core; Herpes Simplex viruses are available from the MIT Viral Core (http://mcgovern.mit.edu/technology/viral-vector); and rabies viruses are available from the Salk Institute Gene Transfer and Therapeutics core (http://www.salk.edu/science/core-facilities/gene-transfer-targeting-and-therapeutics-core/) ! **CAUTION** Follow the appropriate safety precautions pertaining to the particular virus in use. It may be necessary to obtain a higher biosafety level certification before use. ▲ **CRITICAL** Temperature-sensitive viral preparations may not be compatible with delivery from these devices, and thus specific testing should be conducted for each preparation.
- Retrograde tracers (e.g., Cholera Toxin Subunit B[41]; Thermo Fisher, cat. no. C22841) ▲ **CRITICAL** Temperature-sensitive fluids may not be compatible with delivery from these devices. Viscosity affects the flow rate for delivery. If high-viscosity fluids need to be delivered, microfluidic channel dimensions should be engineered to adjust the flow rate accordingly.

EQUIPMENT

Fabrication of optofluidic probes and thermally actuated pumps

- Mask aligner (Karl Suss, MJB series)
- Reactive ion etcher (March Jupiter III RIE, surface activation for PDMS bonding)
- Stereo microscope (Omano, cat. no. OM4713)
- Precision balance (Ohaus, cat. no. NV2101)
- Spin coater (spin coating for SU8, PDMS, and photoresist; Specialty Coating Systems, model no. SCS 6800)
- Desiccator (for polymer degassing before curing; Cole-Parmer)
- Oven (for PDMS curing; VWR)
- Hot plates (Fisher Scientific, cat. no. 11-100-100H)
- FPC cable connectors (Hirose Electric, cat. no. FH34S-6S-0.5SH(50) for ×6 or FH34S-4S-0.5SH(50) for ×4)
- E-beam evaporator (for metal deposition for Au (gold) and Cr (Chrome); AJA International)
- Parylene deposition equipment (for conformal coating of Parylene C; Specialty Coating Systems, SCS Labcoter 2)
- Digital multimeter (Fluke, model no. 115, or other commercially available multimeter)
- Binder clips (Staples, cat. no. 10669)
- Round-edge tweezers (Aven, cat. no. 18049USA)
- Punch, 0.50 mm (Harris Uni-Core)

Preparation of stainless steel for microneedle

- Laser mill (Potomac, model no. LMT-5000S)

Preparation for μ-ILED probes

- Equipment required to prepare μ-ILED probes is described in our previous protocol[35]

Measurement of microfluidic delivery by thermally actuated pumps

- IR camera (for temperature measurement for fluid and thermal actuators; FLIR Systems, model no. A655sc)
- Fluorescent microspheres (for fluid flow rate measurement; Thermo Fisher Scientific, cat. no. F-8827) ! **CAUTION** The diameter of the microspheres should be smaller than the size of the microfluidic channels.
- Digital high-speed camera (for fluid flow rate measurement; Vision Research, model no. Phantom v7.3)
- Inverted optical microscope (Leica) with a 20× objective (Leica) and wide-field fluorescence light source (Excelitas Technologies, model no. X-Cite 120Q)

Preparation of IR wireless modules

- Reflow oven (SMTmax, cat. no. AS-5060)

Preparation of IR wireless receiver

- Flexible printed circuit board (PCB) for wireless receiver modules (PCB Universe, custom design)
- Solder paste (63Sn/37Pb solder paste; Zephyrtronics)
- Microcontroller (Atmel, cat. no. ATTINY84-20MU)
- Current-limiting diode (Semitec, cat. no. S-501T)
- Phototransistor (Optek Technology, cat. no. OP501)
- MOSFET Transistors (Rohm Semiconductor, cat. no. RV1C002UNT2CL)
- Voltage regulator (On Semiconductor, cat. no. NCP4624DMU50TCG)
- IR sensor IC, 38 kHz (Vishay Semiconductors, cat. no. TSOP57438TT1)
- Capacitors, 100 nF (Murata Electronics, cat. no. GRM033R61A104KE15D)
- Resistors, 6.04 k (KOA Speer, cat. no. RK73H1HTTC6041F)
- Resistor, 10 k (KOA Speer, cat. no. RK73H1ETTP1002F)
- Red LED (Vcc, cat. no. VAOL-S4RP4)
- Green LED (Vcc, cat. no. VAOL-S4GT4)
- Lithium ion battery, 3.7 V (PowerStream, cat. no. GM300910H-TUV UL1642)

Preparation of IR wireless remote controller

- PCB (University of Colorado Boulder, custom design)
- Microcontroller (Arduino, model no. Pro mini 328 5 V/16 MHz)
- p-MOSFET (Fairchild Semiconductor, cat. no. FQP27P06)
- Voltage regulator (STMicroelectronics, cat. no. L7800)
- IR LED (Vishay Semiconductor, cat. no. TSTS7100)
- Alkaline battery 9 V (Sparkfun, cat. no. PRT-10218)
- Resistors, 10 k (Sparkfun, cat. no. COM-08374)
- Control buttons (C&K Components)

Preparation of device cases

- 3D printing system (Autodesk, Ember 3D printer)
- 3D CAD tool (Dassault Systèmes, SolidWorks)

Injection of virus and μ-ILEDs into targeted brain structure

- Dual-arm stereotaxic alignment system (e.g., KOPF, model no. 942)
- Stereotaxic drill (KOPF, model no. 1474) and no. 66 drill bit (KOPF, cat. no. 8669)
- Stereotaxic single cannula holder (KOPF, model no. 1766-AP)
- Stereotaxic electrode holder (KOPF, model no. 1770)
- Double-sided Scotch Tape (3M)
- Anchoring screws (CMA Microdialysis, cat. no. 7431021)
- Needles (Becton-Dickinson, cat. no. 305111)
- Scalpel Handle No. 3 (Ted Pella, cat. no. 549-3)
- Scalpel blades (Ted Pella, no. 10: cat. no. 549-3S-10 or no. 11: cat. no. 549-3S-11)
- Forceps (Miltex, cat. no. 6-100)
- Surgical scissors (Miltex, cat. no. 18-1430)
- Hemostats (Miltex, cat. no. MH7-26)
- Microspatula (Chemglass, cat. no. CG-1982-12)
- Electric clippers (Wahl, cat. no. 8064-900)

Behavioral procedures using IR wireless control

- Adult (25–35 g) male or female C57BL/6J mice (Charles River, cat. no. 027), mutant mice (Jackson Laboratory, cat. no. 008601) back-crossed to the C57BL/6J mouse strain, or adult (275–325 g) male Lewis rats (Charles River, cat. no. 004) with an injected optofluidic neural device ! **CAUTION** Before beginning this protocol, the animal care and use committee of the investigating institution should approve all procedures and conform to national guidelines and regulations regarding animal research.
- Relevant behavioral assay apparatus (university machine shops, MED Associates, Harvard Apparatus or other)
- Microcontroller (Arduino UNO, cat. no. ATmega328P)
- Jumper wires (Sparkfun, PRT-08431)
- Alligator clips (Sparkfun, CAB-1319)

REAGENT SETUP

Silk adhesive The silk adhesive can be prepared as described previously[35]. Boil cocoons of the *Bombyx mori* silkworm for 30 min in a solution of 0.02 M Na_2CO_3 to remove the sericin protein. Rinse the extracted fibroin with dH_2O and dry it in ambient air for 12 h. After drying, dissolve the fibroin in a 9.3 M LiBr solution at 60 °C for 4 h, yielding a 20% (wt/vol) aqueous solution, and subsequently dialyze the solution against dH_2O using a dialysis cassette at room temperature for 48 h until the solution reaches a concentration of 8% (wt/vol). The adhesive can be prepared in advance and stored on siliconized paper at room temperature for at least 1 year. The paper can be cut into small strips (~10 × 10 cm) for individual application.

Dental cement The dental cement can be prepared as described elsewhere[16,35]. We recommend 350 µl of methyl methacrylate monomer added to 225 mg of dental cement powder. ▲ CRITICAL STEP Adjusting the viscosity alters the working time of the cement. Each user should adjust the viscosity (by increasing or decreasing the amount of methyl methacrylate in the mixture) to properly achieve the optimal working time. The cement must be prepared immediately before use and will only allow a few minutes of working time before curing.

ACSF The most important aspect of the ACSF is that it is a biologically compatible aqueous solution for dissolving the silk adhesive. The solution can be prepared according to recipes described elsewhere[14,69,70]. We recommend a solution that is 300–310 mOsm. The ACSF can be prepared in advance and stored in bulk for many months at 4 °C, so long as it is handled carefully to maintain sterility.

EQUIPMENT SETUP

Preparation of the electrode holder for removal of the microneedle

Carefully align a fresh piece of double-sided tape with the bottom edge of the electrode holder (KOPF, model no. 1770). Be careful not to touch the tape or allow it to gather dust, in order to ensure maximum adhesiveness.

PROCEDURE

Preparation of flexible µ-ILED probes ● TIMING 7 d

1| Follow Steps 1–18 of the previous protocol[35] to prepare flexible µ-ILEDs probes.

Fabrication of ultrathin, flexible microfluidic channels ● TIMING 3 d

2| *Microfluidic channel preparation* (**Fig. 1** and **Supplementary Fig. 1**). Degrease large glass slides (3 inches × 2 inches) with acetone/isopropyl alcohol (IPA)/deionized water (DI) water/IPA, nitrogen-blow to dry them, and bake them on a 110 °C hot plate for 1 min to dehydrate.

3| Prepare Pt (freely diffusing catalyst) inhibition solution with 5% (wt/wt) [3-(2-aminoethylamino)propyl]trimethoxysilane (AEAPS) and 95% (wt/wt) methanol (e.g., 5 g of AEAPS and 95 g methanol; **Fig. 1a**).

4| Immerse degreased glass slides in the inhibitor solution for 45 min to activate the glass surface with Pt inhibitor, which prevents polydimethylsiloxane (PDMS) polymerization at the glass–PDMS interface (**Fig. 1b**, **Supplementary Fig. 1a**). This step ensures nondestructive release of the PDMS layer from the glass surface.

5| Rinse both sides of the slide with methanol and dry it on a hot plate at 70 °C for 15 min (**Fig. 1c**,**d**, **Supplementary Fig. 1b**).

6| In the meantime, make the microfluidic channel mold using UV-curable epoxy (SU-8 10). The design for microfluidic channels is shown in **Supplementary Figure 2** and **Supplementary Data 1**. Spin-coat UV-curable epoxy onto a silicon wafer at 3,000 r.p.m. for 30 s to produce a 10-µm-thick layer. Next, prebake it at 65 °C for 2 min, 75 °C for 2 min, 85 °C for 2 min, 95 °C for 5 min, and 65 °C for 2 min, and UV-expose (120 mJ/cm^2) it through a mask pattern (Mask 1; mask for microfluidic patterns; **Supplementary Data 1**). Postbake the wafer sample sequentially on a hot plate at 65 °C for 1 min, 75 °C for 1 min, 85 °C for 1 min, and 95 °C for 2 min. Next, eliminate the epoxy in the unexposed region by developing with SU-8 developer.

7| Repeat Step 6 with Mask 2 (mask for spacer patterns; **Supplementary Data 1**). This process creates a 20-µm-thick spacer only at the boundary of the mold, thus allowing creation of microfluidic channel patterns with one side closed (**Fig. 1e**, **Supplementary Fig. 1d**).

8| Mount a small beaker on the inner wall of a wafer box and add anti-stiction agent (chlorotrimethylsilane (TMCS)) to the beaker. Put the mold wafers in the box and completely seal the box. Next, place the box in the fume hood and wait for 20 min to allow evaporation of the anti-stiction agent onto the surface of the mold wafer (**Fig. 1f**, **Supplementary Fig. 1e**). This process facilitates the release of patterned PDMS from the mold later.

9| Mix PDMS elastomer and curing agent with a 10:1 weight ratio and degas in a vacuum chamber for ~30 min.

10| Cast PDMS on the mold and press it with the glass substrate prepared in Steps 2–5. Clamp the mold and the glass slide together using binder clips and cure in a 70 °C oven for 50 min (**Fig. 1g–j**, **Supplementary Fig. 1c**,**f**,**g**).
▲ CRITICAL STEP Press the mold hard with the glass substrate to spread the PDMS uniformly.

11| Carefully release the glass substrate with the patterned PDMS layer from the mold in preparation for bonding to a cover PDMS layer (**Fig. 1k**,**l**, **Supplementary Fig. 1h**).
? TROUBLESHOOTING

12| *Cover layer preparation*. On a separate glass substrate, attach a polycarbonate (PC) sheet with tape (**Fig. 1m**, **Supplementary Fig. 1i**). PC does not allow strong bonding of silicone to its surface, thus facilitating release of the PDMS.

13| Cast PDMS (elastomer/curing agent ratio = 10:1) on the PC substrate, spin-coat at 2,000 r.p.m. for 60 s for a 20-µm-thick flat PDMS layer, and cure at 70 °C for 1 h (**Fig. 1n**, **Supplementary Fig. 1j**,**k**).

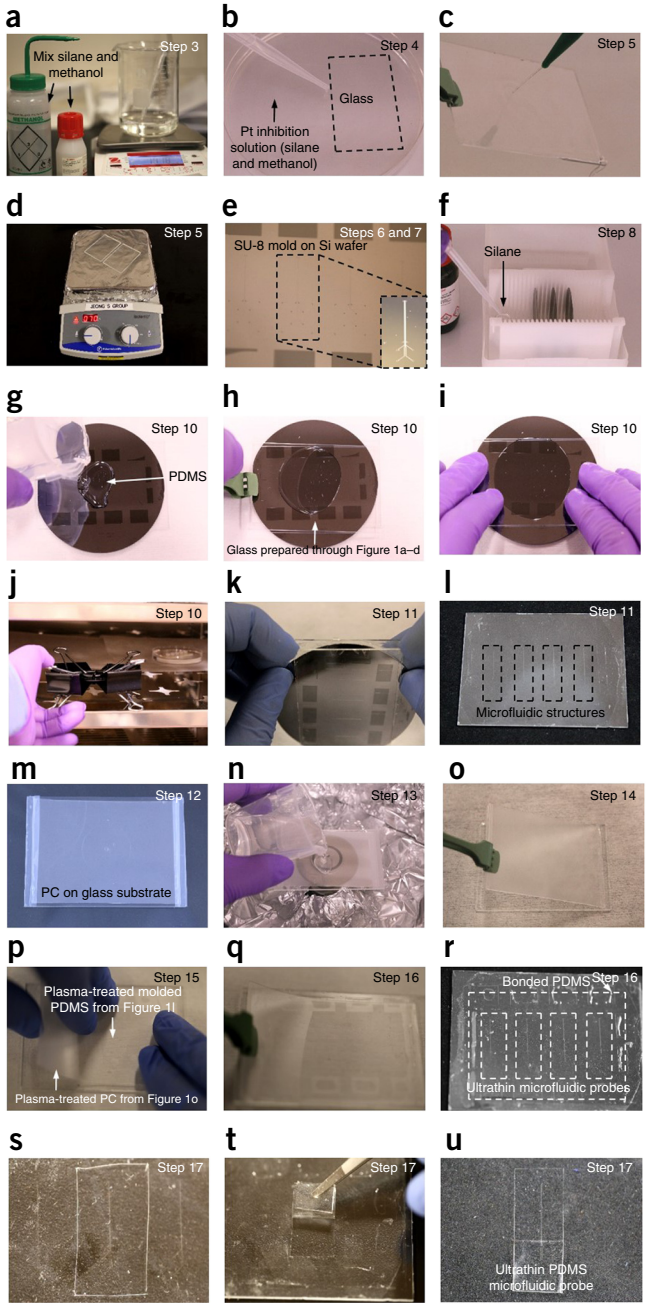

Figure 1 | Fabrication process for ultrathin, flexible microfluidic channels. (**a**) Prepare Pt (freely diffusing catalyst) inhibition solution with 5% (wt/wt) AEAPS and 95% (wt/wt) methanol (e.g., 5 g of AEAPS and 95 g of methanol). (**b**) Immerse degreased glass slides in the inhibitor solution to activate the glass surface with Pt inhibitor. (**c**) Rinse both sides of the slide with methanol. (**d**) Dry the slide on a hot plate at 70 °C for 15 min. (**e**) Make the microfluidic channel mold using UV-curable epoxy (SU-8 10). (**f**) Perform anti-stiction surface treatment on the mold wafer by evaporating anti-stiction agent (TMCS) in a completely enclosed wafer box. (**g**) Cast PDMS on the mold. (**h–j**) Press and clip the PDMS-casted mold to the glass substrate and cure it at 70 °C for 1 h. (**k**,**l**) Carefully release the glass substrate with the patterned PDMS layer from the mold in preparation for bonding to a cover PDMS layer. (**m**) On a separate glass substrate, attach a polycarbonate (PC) sheet with tape. (**n**) Cast PDMS (elastomer/curing agent ratio = 10:1) on the PC substrate, spin-coat at 2,000 r.p.m. for 60 s to obtain a 20-μm-thick flat PDMS layer and cure at 70 °C for 1 h. (**o**) Cut the PDMS-coated PC sheet to the proper size for release from the glass substrate in preparation for bonding. (**p**) Activate the surfaces of the flat PDMS on the PC sheet and the patterned PDMS on the glass slide with oxygen–plasma in March Jupiter III RIE and bond them together. (**q**,**r**) Delaminate the PC sheet from the bonded PDMS. (**s–u**) Carefully detach the bonded PDMS layer from the glass substrate to obtain ultrathin, flexible PDMS microfluidic devices.

14| Upon curing, cut the PDMS-coated PC sheet to the proper size for release from the glass substrate in preparation for bonding (**Fig. 1o**).

15| *Bonding and release.* Activate the surfaces of the flat PDMS on the PC sheet and the patterned PDMS on the glass side with oxygen–plasma in March Jupiter III RIE (pressure: 0.9 torr; O_2 flow rate: 4 sccm; RF power: 45 W; time: 50 s) and bond them together (**Fig. 1p**, **Supplementary Fig. 1m**). ▲ **CRITICAL STEP** Place the bonded sample on a hot plate and bake it at 70 °C for >4 h to enhance bonding quality. ■ **PAUSE POINT** The sample can be left overnight on a hot plate at 70 °C.

16| Delaminate the PC sheet from the bonded PDMS (**Fig. 1q**,**r**, **Supplementary Fig. 1n**).

17| Carefully detach the bonded PDMS layer from the glass substrate using a tweezer and obtain ultrathin, flexible PDMS microfluidic devices (**Fig. 1s–u**, **Supplementary Fig. 1o**,**p**). The PDMS can be smoothly released from the glass substrate without damage, assisted by the amine groups on the glass surface that bind and deactivate the Pt in the interfacial PDMS prepolymer. **Figure 2a** shows a released microfluidic device layer (50 μm thick).

Preparation of a microfluidic probe and integration with a μ-ILED probe ● **TIMING 1 h**

18| Cut away the unnecessary PDMS part with a custom-designed blade tool to create a small (500-μm-wide) microfluidic neural probe (**Fig. 2b**,**c**). The tool has two blades separated by 500 μm to facilitate the creation of small probes (**Supplementary Fig. 3a**, **Supplementary Data 2**).
! **CAUTION** Be careful not to damage the microfluidic channels during cutting.

19| Create vertical fluidic channels that are connected to horizontal microfluidic channels in the probe. Fluids from the reservoirs will pass through the vertical channels to the microfluidic probe when pumped out. First, place a 3D-printed alignment tool (**Supplementary Fig. 3b**, **Supplementary Data 3**) for a punch (Harris Uni-Core, 0.50 mm, **Supplementary Fig. 3c**) on the four ends of the microfluidic channels, as shown in **Figure 2d**. Then, make punch holes by inserting and pressing the punch through the four alignment holes (**Fig. 2e**).

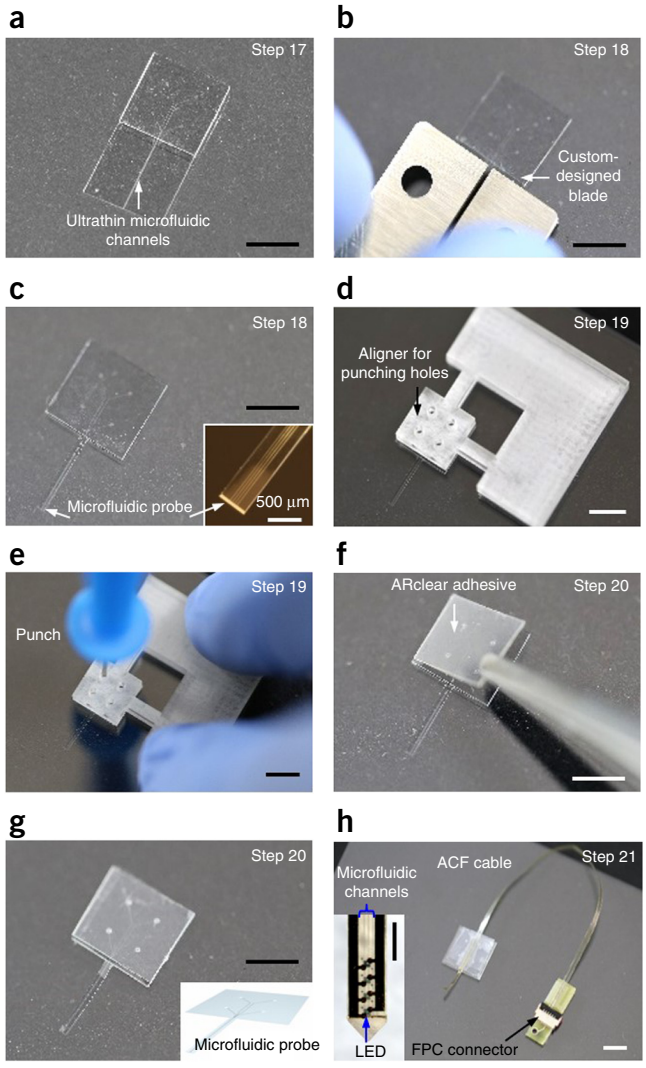

Figure 2 | Procedure for creating the optofluidic probe. (**a**) Place the ultrathin PDMS microfluidic channel device onto a glass slide. (**b**) Cut the PDMS device with a blade to form a 500-µm-wide microfluidic probe. (**c**) Photographs demonstrating the resulting microfluidic probe. (**d**) Place a 3D-printed aligner on the PDMS device to guide a punch tool to create vertical fluidic channels at the precise positions of the microfluidic channel ends. The aligner has four holes that a punch can enter. (**e**) Mechanically punch holes. Vertical channels formed in this manner connect to horizontal microfluidic channels in the probe. (**f**) Attach adhesive film to one side of the device to block one end of the vertical fluidic channels. This creates L-shaped fluidic channels in the microfluidic probe. (**g**) Photograph and schematic of the resulting microfluidic device layer. (**h**) Attach an LED probe on top of the microfluidic probe using adhesive film to form an optofluidic probe. (Inset) Magnified view of the optofluidic probe (scale bar, 500 µm). All scale bars are 5 mm unless otherwise noted. ACF, anisotropic conductive film.

20| Attach the adhesive film (ARclear 8154) to one side of the device where the punch holes are located (**Fig. 2f**,**g**). The film blocks one end of the vertical fluidic channels, therefore guiding the fluid flow to the horizontal microfluidic channels in the probe (**Supplementary Fig. 4**).

21| Mount an LED probe on top of the microfluidic probe using adhesive film (ARclear 8154) to create an optofluidic probe (**Fig. 2h**). If you need fluid delivery only, skip this step.
▲ **CRITICAL STEP** Both the microfluidic and LED probes are small (500 µm wide, 7 mm long). This step should be done under the microscope to avoid misalignment between the two probes.

Fabrication of thermally actuated pump ● **TIMING 2 d**
22| Deposit a Cr/Au layer (5 nm/185 nm) on the FR-4 substrate (**Fig. 3a**) using an e-beam evaporator.
▲ **CRITICAL STEP** Find the optimal metal thicknesses that provide the maximum power efficiency for the design of your microheaters.

23| Photolithographically pattern the Cr/Au layer using a positive photoresist (AZ5214E). First, spin-coat the photoresist (AZ5214E) for 30 s at 3,000 r.p.m. and bake it on a hot plate (110 °C) for 1 min. UV-expose (total energy of 130 mJ/cm^2) through a mask (for microheater patterns; **Supplementary Fig. 5**, **Supplementary Data 1**) and develop with AZ 917MIF for ~25 s. Next, etch Cr and Au for ~10 s and 45 s, respectively (5 nm and 185 nm of Cr and Au, respectively. Etch time varies with metal thicknesses). Finally, remove the photoresist with acetone/IPA to complete fabrication of the microheaters (**Fig. 3b**).
▲ **CRITICAL STEP** Measure the resistance of the heater to ensure that there is an electrical connection in the metal traces.
? TROUBLESHOOTING

24| Prepare the expandable composite material by mixing PDMS (elastomer/curing agent ratio = 10:1) and expandable microspheres (Expancel microspheres) with a weight ratio of 2:1. Cover the contact pads of the heaters with thin PDMS pieces (<1 mm thick) to keep them from being coated by the expandable composite material and Parylene C. Next, spin-coat this composite material onto the microheaters for 60 s at 500 r.p.m. and cure them in a 70 °C oven for 12 h to form an expandable layer (250 µm) that can be actuated by Joule heating (**Fig. 3c**,**d**).
■ **PAUSE POINT** They can be left in a 70 °C oven for a few days.

25| Create hemispherical reservoirs (0.5 µl volume) and vertical microfluidic channels (450-µm diameter) by milling a 2-mm-thick plastic slab (**Fig. 3e**, **Supplementary Fig. 6**). Depending on the light sensitivity of the fluids that will be used for the experiments, this step can be performed using milling cyclic olefin polymer (COP), which is transparent and has very low water vapor permeability (0.023 g·mm/m^2·day), for light-insensitive compounds or black plastic slab, which can block UV and visible light (e.g., IR-transmitting sheets available from ePlastics), for light-sensitive compounds.

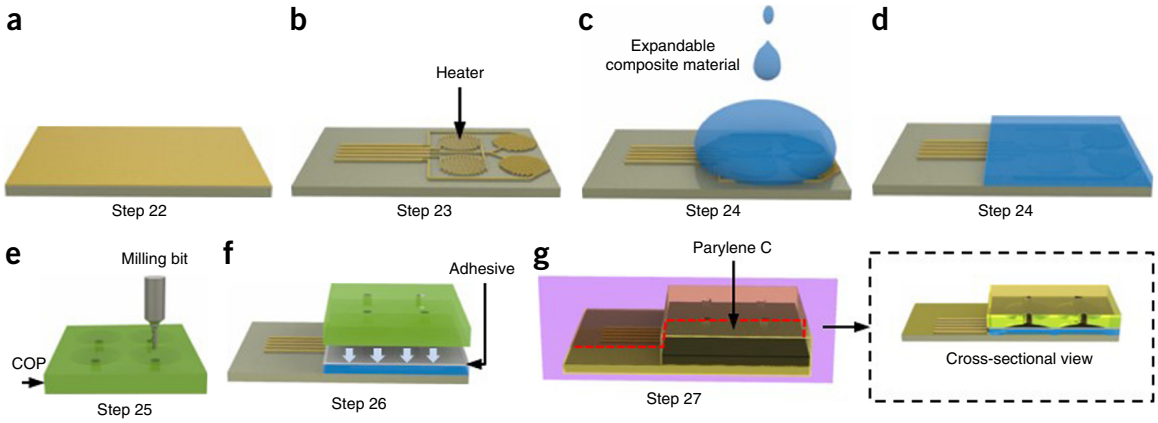

Figure 3 | Schematic showing fabrication procedure for thermally actuated pumps. (**a**) Deposit Cr/Au layer (5 nm/185 nm) on a FR-4 substrate using an e-beam evaporator. (**b**) To create microheaters, perform photolithography to pattern the Cr/Au layer. (**c**) Prepare the expandable composite material by mixing PDMS and expandable microspheres with a weight ratio of 2:1 and cast the material on the microheaters. (**d**) Spin-coat the composite material and cure it at 70 °C for 12 h to form a thermally expandable layer with a thickness of 250 μm. (**e**) Make hemispherical reservoirs and vertical microfluidic channels in a 2-mm-thick COP slab by milling. (**f**) Align and mount the COP reservoir slab on the expandable layer using adhesive film. (**g**) For long-term fluid storage, deposit Parylene C (6 μm thick) on the inner walls of the reservoirs to prevent fluid evaporation.

26| Align the four reservoirs precisely on the heaters and adhere them to the expandable layer using double-sided polyester film (ARclear 8154) (**Fig. 3f**).

27| Make a conformal deposition of Parylene C (6 μm thick) using an SCS Labcoter 2 on the inner surface of the reservoirs to ensure vapor impermeability through the reservoir walls and the expandable layer (**Fig. 3g**).

Fluid loading and final assembly ● TIMING <1 h

28| Delaminate the PDMS pieces to expose the contact pads for an electrical connection. Using silver epoxy, attach an FPC connector to the contact pads of the thermally actuated pump. This connector allows the wireless receiver module to be easily plugged in (**Fig. 4a**,**b**). Use 5 Minute Epoxy to permanently mount the FPC connector on the FR-4 substrate.
? TROUBLESHOOTING

29| The inner walls of the reservoirs are hydrophobic because of the Parylene coating. To facilitate fluid loading, treat the reservoirs with oxygen plasma (March Jupiter III RIE; process condition: 300 mTorr/200 W/30 s/20 sccm O_2) to make the inner-wall surface hydrophilic.

30| Load fluids with a blunt syringe needle (26 gauge) in each reservoir and attach double-sided adhesive film (ARclear 8154) to the tops of the reservoirs (**Fig. 4c–e**).

31| Mount copper membranes (3 μm in thickness) on the four posts of a PDMS stamp and print them on the outlets of the reservoirs for a complete seal to prevent fluid evaporation (**Fig. 4f–h**).

32| Assemble the optofluidic probe from Step 21 onto the pump, with careful alignment between the vertical fluidic channels of the microfluidic probe and the pump (**Fig. 4i**).
▲ CRITICAL STEP Drawing alignment marks at the four corners of the COP reservoir, to indicate the positions of their vertical fluidic channels, enables precise alignment between the vertical fluidic channels of the microfluidic probe and the pump.

Preparation of IR wireless control modules ● TIMING 1 d

33| Design and build thin, flexible PCBs for IR wireless control modules to enable wireless control of fluid delivery and photostimulation (**Supplementary Fig. 7**). The flexible PCB substantially reduces the device weight, as compared with that of a standard, rigid PCB. Flexible PCBs can be constructed using PCB vendors or can be custom-fabricated on a thin Kapton film[35] (**Fig. 5a**).

34| Using a microscope, place solder paste on the PCB electrodes and mount the electronic components (a microcontroller (ATTINY84-20MU, Atmel), transistors, an IR detector (IR Sensor IC, 38 kHz, Vishay Semiconductors), current-limiting diode, voltage regulator, and so on), according to the circuit diagram (**Fig. 5b**, **Supplementary Fig. 7**).

35| Cure solder paste in the reflow oven (**Fig. 5c**). **Figure 5c** inset shows a completed wireless receiver module, which is ready to be connected to an optofluidic device and rechargeable lithium ion batteries (GM300910H, PowerStream Technology).

36| Construct a remote controller using two microcontrollers (Pro mini 328 5 V/16 MHz, Arduino), IR LED (950-nm wavelength, TSTS7100, Vishay Semiconductor), control buttons, resistors, and voltage regulators (**Fig. 5d**). The circuit diagram for the controller can be found in **Supplementary Figure 7**. Use a 9-V battery to operate the remote controller.

Preparation of plastic device cases ● TIMING 1 d

37| Design the 3D-printed enclosure using a 3D CAD tool (SolidWorks) to completely enclose the batteries and flexible PCB (**Supplementary Data 4** and **5**). Print this design using a stereolithography system (Ember 3D printer, Autodesk) with a clear epoxy-based photopolymer for rapid prototyping.

Implantation of optofluidic probe into targeted brain structure ● TIMING 1 d

38| To prepare the animal for implantation, carefully follow Steps 24–38 of our previous protocol[35].

▲ CRITICAL STEP Before beginning this protocol, all procedures should be approved by the animal care and use committee of the investigating institution and conform to national guidelines and regulations regarding animal research.

? TROUBLESHOOTING

39| Sterilize the probe. For implantation into rodents, rinse with ethanol to sterilize the device before injection. For other mammals and primates, it might be necessary to use room-temperature ethylene oxide gas sterilization (http://www.anpro.com/sterilizers/anprolene/indexanprolene.html).

? TROUBLESHOOTING

40| Mount the optofluidic neural probe in the cannula holder. If you are planning on removing the microneedle, position the microfluidic neural probe as shown in **Figure 6a**; if you are leaving the microneedle attached, position the microfluidic neural probe as shown in **Figure 6b**. The probe must be parallel to the midline of the cannula holder to achieve proper spatial targeting (**Fig. 6c**).

? TROUBLESHOOTING

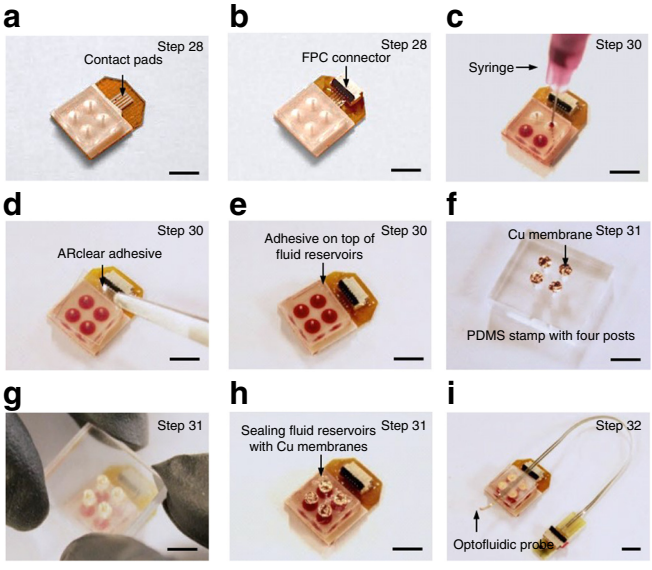

Figure 4 | Procedure for drug loading and assembly with an optofluidic probe. (**a**,**b**) Attach an FPC connector to the contact pads of the thermally actuated pump. (**c**) Treat the device with oxygen plasma to make the inner walls of the reservoirs hydrophilic and inject fluids into each reservoir with a blunt syringe needle (26 gauge). (**d**,**e**) Attach adhesive film to the reservoirs. (**f**) Mount Cu membrane pieces on four posts of a PDMS stamp. (**g**,**h**) Transfer-print the Cu membrane on the reservoirs to seal the fluid outlets. (**i**) Integrate an optofluidic probe onto the pump with a careful alignment between vertical fluidic channels of the microfluidic probe and the pump. The device is now ready to use. Scale bars, 5 mm.

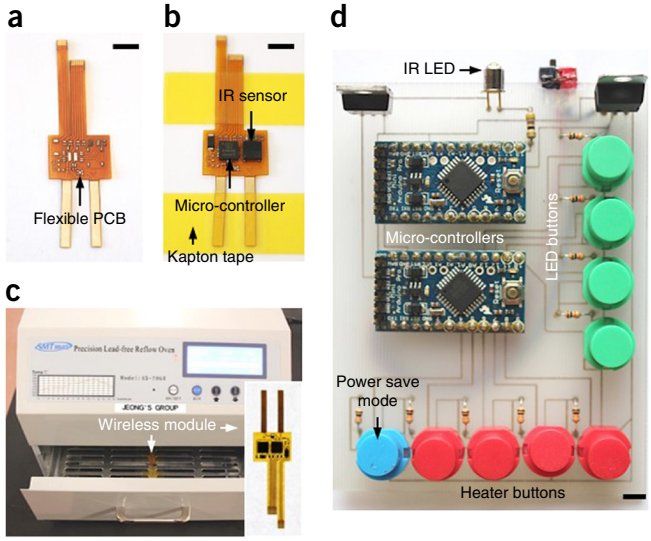

Figure 5 | Preparation of IR wireless control modules. (**a**) Photograph of a flexible PCB for the wireless receiver before mounting the chips. (**b**) Put solder paste on the electrodes and mount the electronic components, including a microcontroller and an IR sensor. (**c**) Cure solder paste in the reflow oven to complete the wireless receiver. The inset shows a completed wireless receiver. (**d**) Photograph of a wireless remote controller that sends commands to the wireless receiver when buttons are pressed. Scale bars, 5 mm.

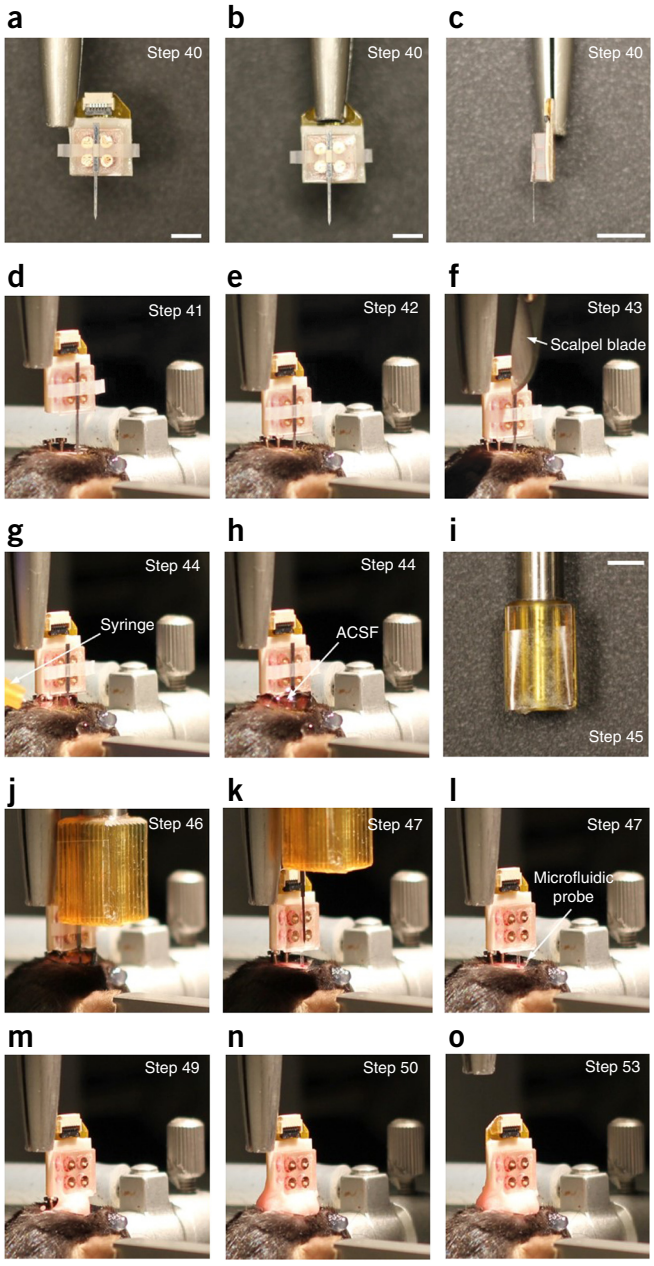

Figure 6 | Surgical procedure for implantation of the optofluidic neural probes into the brain. (**a**) A microfluidic neural probe attached to the cannula holder in the optimal position for removal of the microneedle. (**b**) A microfluidic neural probe attached to the cannula holder in the optimal position for permanent implantation of the microneedle. (**c**) Note the alignment of the optofluidic probe with the cannula holder. (**d**) An optofluidic neural probe ready to be inserted into the brain through a prepared craniotomy. (**e**) The optofluidic probe is lowered to the target depth. (**f**) The tape affixing the microneedle is severed with a scalpel blade. (**g**) ACSF is applied to optofluidic neural probe and the skull surface to dissolve any external silk adhesive. (**h**) ACSF is accumulated for 15 min on the base of the skull. (**i**) The electrode holder is prepared with properly clean and aligned double-sided tape (see Equipment Setup). (**j**) The electrode holder is positioned adjacent to the microneedle. (**k**) The electrode holder is used to carefully retract the microneedle from the skull. (**l**) The needle is completely removed, leaving only the ultrathin microfluidic channels. (**m**) Dental cement is applied directly to the craniotomy site to secure the optofluidic neural probe in its targeted position. (**n**) The remainder of the headcap is formed from dental cement, taking care to ensure that no bonds are made directly to the soft tissue. (**o**) The cannula holder is removed, leaving the optofluidic neural probe stably implanted. All procedures were approved by the Animal Care and Use Committee of Washington University and conformed to US National Institutes of Health guidelines. Scale bars, 5 mm.

41| Position the cannula holder such that the optofluidic probe is above the drill hole (**Fig. 6d**). If applicable, take care to orient the μ-ILED in the direction suitable for the experiment in order to properly illuminate the opsin-expressing brain region of interest. The microfluidic channels expel fluids ventrally, so target them dorsally to your site of interest.

42| Slowly lower the device into the brain to the desired dorsal–ventral coordinates (**Fig. 6e**). If you are planning on removing the microneedle, continue to Step 43; if you are leaving the microneedle attached, skip to Step 48.

43| Carefully make two incisions in the single-sided tape affixing the microneedle to the fluid chambers to separate it from the rest of the device (**Fig. 6f**).
▲ **CRITICAL STEP** Always use a fresh scalpel blade to ensure maximum sharpness. Any movement that does not cut the tape will cause excess damage to the tissue.
▲ **CRITICAL STEP** Practice this step before surgery. A practiced hand can complete this task without error every time.
? TROUBLESHOOTING

44| Using a syringe needle, slowly apply ACSF to the skull to dissolve the external silk-based adhesive. Be sure to run ACSF across any region of the needle that makes contact with the probe and chamber casing (**Fig. 6g**). Try to accumulate as much ACSF as possible in a pool resting on the skull. The brain tissue will dissolve the adhesive inside the skull. Wait at least 10 min to allow for complete dissolution of the adhesive (**Fig. 6h**).
▲ **CRITICAL STEP** The adhesive must be completely dissolved before microneedle removal. If not, the final placement will be affected.

45| Mount the prepared electrode holder (**Fig. 6i**) (Equipment Setup) on the second arm of the stereotax.

46| Position the electrode holder immediately adjacent to the exposed microneedle (**Fig. 6j**).

47| Without any medial–lateral or anterior–posterior movement, slowly remove the microneedle along the dorsal–ventral axis (**Fig. 6k**). Monitor the position of the flexible substrates to ensure that zero movement occurs. If the adhesive is completely dissolved, the microneedle will be removed with ease and without movement (**Fig. 6l**).

48| Prepare the dental cement according to the instructions in the Reagent Setup.

49| Using a microspatula, carefully apply a layer of dental cement directly to the point of injection to fully secure the placement of the flexible device (**Fig. 6m**).
▲ **CRITICAL STEP** Wait for 2–5 min to allow this layer of cement to completely cure before building the structure of the remaining headcap. Gently tap the cement with a spatula to determine that it is has hardened and fully cured.

50| Once the initial layer of cement is fully cured, continue to build the headcap in a manner that secures the entire base of the implant (**Fig. 6n**).
▲ **CRITICAL STEP** Be careful to encompass only enough—but not too much—of the base to secure it, to ensure that the control casing will still affix properly to the implanted hardware.

51| Use a sterile spatula to detach any scalp skin from the cement. If the skin and the cement are connected, the headstage will be less stable over time and more prone to infection.

52| Liberally apply ~1 g of the antibiotic ointment and lidocaine ointment to the entire incision area.

53| Once the full headcap has cured and the scalp has been treated, release the grip of the cannula holder and raise it away from the animal along the dorsal–ventral axis (**Fig. 6o**).

54| Remove the animal from the stereotaxic frame and place it in a clean home cage position on top of a heating pad for recovery. The animal should recover rapidly (<15 min) and can be returned to its home cage once it displays normal, awake locomotor behaviors.

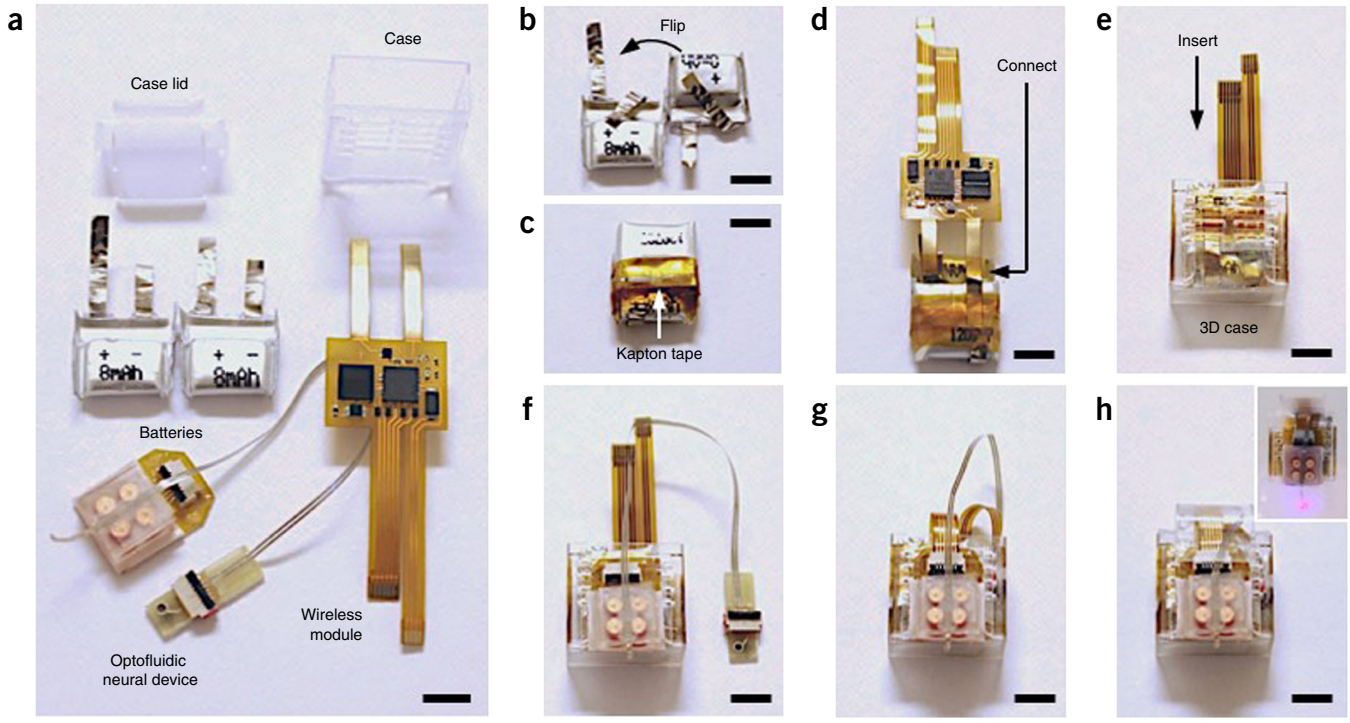

Figure 7 | Device integration for an entirely self-contained wireless drug delivery system. (**a**) Photograph of an optofluidic neural device, a wireless control module, two batteries, and a device case that are integrated for the wireless microfluidic neural probe system. (**b**–**h**) System assembly process. (**b**) Prepare two lithium ion batteries. (**c**) Make a serial connection of batteries and secure tightly with Kapton tape. (**d**) Connect the wireless module to the batteries. (**e**) Wrap the wireless module around the batteries, securing tightly with Kapton tape. Insert the wireless module and batteries into the plastic case. (**f**) Slide the optofluidic neural device into the case. (**g**) Plug the cables of the wireless module into the neural device: one for the heater control and the other for the LED control. (**h**) Cover the case with the lid for protection. (Inset) Photograph of a wireless optofluidic neural probe system that offers both fluid and photostimulation independently. Scale bars, 5 mm.

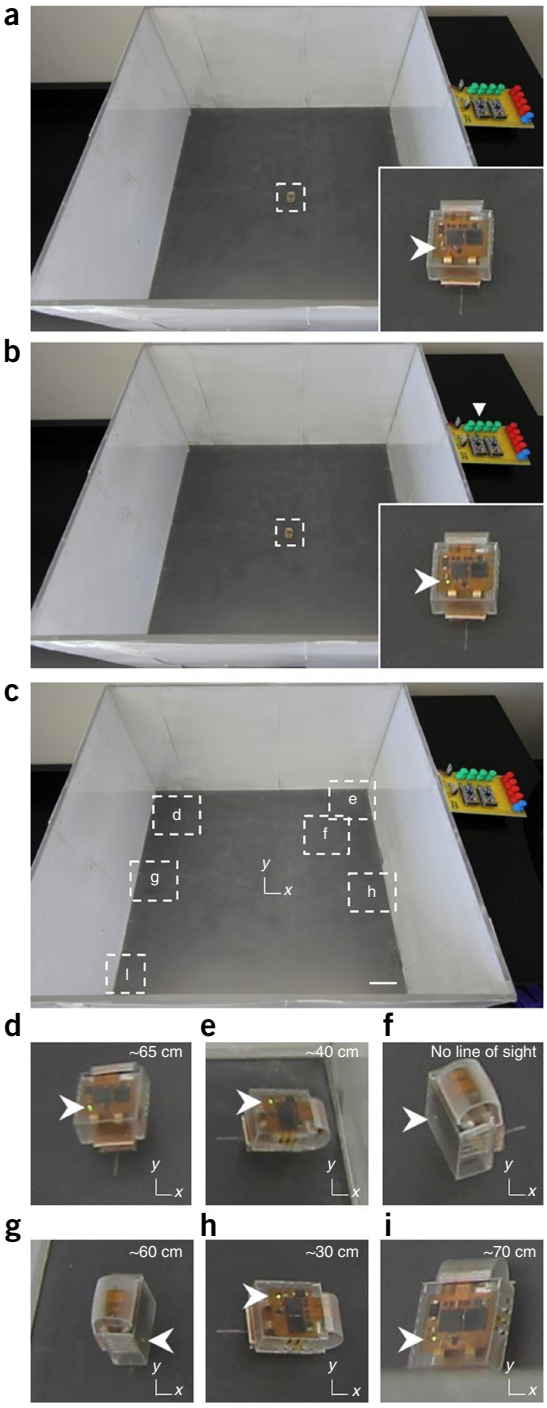

Figure 8 | Example preparation of the behavioral assay for wireless control. (**a**) The IR remote is positioned <1 m from the behavior arena, in this case a 50 × 50 cm open field. A complete microfluidic device is placed in the center of the field. Inset, the indicator LED on the wireless control module is off (arrowhead). (**b**) The wireless control module is activated after the pressing of one of the LED control buttons on the IR remote (triangle). Inset, the indicator LED on the wireless control module is on (arrowhead). (**c**) The testing microfluidic device is placed in various orientations in many different positions throughout the open field. At each example position (labeled by the letters, d–i, corresponding to the panels below), the same button on the IR remote is pressed and the activation of the indicator LED on the wireless control module is monitored. (**d**–**i**) The device is activated in every test position (arrowheads), including positions at the far side of the arena (**d**,**g**,**i**), as well as orientations without direct line of sight (**e**,**f**,**h**). The noted distances are the approximate spacing between the IR emission LED and the receiver on the wireless control module. The physical orientations of the *x* and *y* axes are consistent across **c**–**i** and are used here to demonstrate relative positioning of the wireless control module as compared with that of the IR remote.

55| The stainless steel microneedle should be clear of any components of the device. Remove from the electrode holder adaptor and sterilize for reuse as described in Box 2 of our original protocol[35].

Animal preparation for behavioral testing ● TIMING 1–7 d

56| House mice until they have recovered from surgery and are ready for behavioral testing. This duration will depend largely on the type of experiment, but in general it is best to perform any fluid delivery within 7 d of implantation to avoid significant volume loss by evaporation. Optical stimulation can occur at any relevant time point with access to a charged battery.

▲ **CRITICAL STEP** If the behavioral experiment is dependent on a prior viral injection (as described in Steps 36–38 of our original protocol[35]), then the timing of the device implantation should account for this time delay. This duration will vary from a few days to 6 weeks, depending on the virus being expressed.

57| If the behavioral assay will involve physical handling of the animals, habituate the animal to handling at least 5 d before experimentation to reduce stress and to ensure smoother operation on the test day. Specifically, handle the animals and adjust the hardware as will be necessary for the experiment. If the entire experiment will be performed wirelessly (i.e., no physical interaction with the animal), then this step can be skipped.

58| In addition, habituate the animals to the method of powering the devices. If an acute mounting of the wireless control module is being used, then acutely affix the casing for at least 20 min once a day for 3 d. If a fully self-contained approach is used, then the animal will habituate over time on its own within 1–3 d.

▲ **CRITICAL STEP** To eliminate locomotor confounding, the animals must be habituated to carrying the added weight of the powering module.

Device integration for an entirely self-contained system ● TIMING 5 min

59| For assembly of an entirely self-contained wireless neural probe system, first connect two batteries in series using Kapton tape (**Fig. 7a–c**). See **Figure 7a** for device components, including a microfluidic neural probe device, an IR-based wireless module, two lithium ion batteries (GM300910H, PowerStream Technology), and a 3D-printed plastic case. The details about the wireless control system can be found elsewhere[36,71].

Box 1 | Providing of external control of the IR remote ● TIMING 1 h

One particularly compelling application of these devices is in behaviorally closed-loop interrogation of neural circuit function. In such cases, the user will want to yield control of the IR remote to a programmed control system (e.g., an I/O box from behavioral software, external function generator, external timing system, and so on). Doing so is both easy and reversible. This case demonstrates how the IR remote can be adapted for control by a microcontroller gated by feedback from the animal's behavior.

Procedure

1. Turn the power switch on the IR remote to the OFF position.
2. Load the desired control sketch onto the Arduino UNO. An example sketch that functions as a triggered function generator is provided in the **Supplementary Note**.
3. Using the jumper cables, connect the triggering source (e.g., TTL signal from behavioral software) to a GND (ground) and Pin 2 of the Arduino UNO (**Fig. 9a**).
4. Plug the alligator clips into another GND and Pin 13 (**Fig 9a**).
5. Connect the alligator clips to the leads under the button that represents the desired feature to be externally controlled (**Fig. 9b**). The microcontroller should now provide triggered function of the IR remote.
6. Repeat steps 2–5 as many times as necessary to control more functions.
7. Turn the power switch on the IR remote to the ON position.

▲ CRITICAL STEP The remote must be within ~10 cm of the wireless module to bring it out of standby mode.

8. Use the blue button on the IR remote to bring all relevant optofluidic probes out of standby mode.
9. Place the animal in the behavior arena with the IR remote in a functional position to activate the wireless module and begin the trial.

60| Electrically connect the wireless module with batteries and insert them into the 3D-printed case (**Fig. 7d**,**e**). Test the wireless module with a remote controller to ensure that there is an electrical connection to the batteries.
? TROUBLESHOOTING

61| Slide the optofluidic device into the top groove of the case (**Fig. 7f**).

62| Plug the control cables of the wireless module into the microfluidic and LED connectors to enable wireless control of fluidic delivery and photostimulation (**Fig. 7g**).
▲ CRITICAL STEP This connection must be properly aligned. The pins of the cable should align with the teeth of the connector, and the cable should be straight upon entering the connector. To ensure proper function of an optofluidic device, test the μ-ILED function at this step.
? TROUBLESHOOTING

63| Finally, cover the wireless module, the batteries, and the cable with a plastic lid for protection (**Fig. 7h**), and attach the lid to the case using 5 Minute Epoxy to prevent potential damage.

Preparation of the behavioral assay for wireless control ● TIMING 1 d

▲ CRITICAL Before beginning the behavioral experiment, it is essential to actively test the optimal location of the IR remote in relation to the behavioral arena. Turn the power switch on the IR remote to the ON position.

64| Use the blue button on the IR remote to bring the test wireless control module out of standby mode.
▲ CRITICAL STEP The remote must be within ~10 cm of the wireless module to bring it out of standby mode.

65| Place the IR remote within ~1–2 m of the behavior arena to be tested (**Fig 8a**,**b**).
? TROUBLESHOOTING

66| Place the prepared wireless module at every conceivable position and angle the animal may be in during the time frame in which communication with the IR remote is needed. At each location, press a function button on the IR remote and determine (via the indicator LEDs (green for μ-ILED operation and red for Joule heater operation) on the wireless control electronics) whether the signal was received. Despite the IR LED and the IR receiver having predetermined emission angles and sensitivities, respectively, we have found that reliable operation is easily achieved in most behavioral assays regardless of a direct line of sight or a particular angle. This ease of operation is due to the reflection and scattering of the IR signal (**Fig 8c–i**).
? TROUBLESHOOTING

67| Once proper function of the wireless control electronics is confirmed by observation of the indicator LEDs within the behavioral arena, permanently place the IR remote at the testing location or otherwise mark the location for future use.

68| Prepare any relevant behavioral testing software and hardware. If device function should be directly controlled by the animal's behavior, follow the instructions in **Box 1**, the **Supplementary Note**, and **Figure 9** to provide external, automated control of the IR remote.
▲ **CRITICAL STEP** Optofluidic probes are compatible with most behavioral acquisition software, including ANY-Maze[72], EthoVision[73], Med Associates[65], and custom packages[74]. Follow related methods and protocols to ensure proper behavioral data acquisition[21,22,36,65,72–77].

69| Use the blue button on the IR remote to place the test wireless control module into power-saving mode.

70| Turn the power switch on the IR remote to the OFF position.

Behavioral testing ● **TIMING 1–7 d**
71| Turn the power switch on the IR remote to the ON position.

72| Use the blue button on the IR remote to bring all relevant optofluidic probes out of standby mode.
▲ **CRITICAL STEP** The remote must be within ~10 cm of the wireless module to bring it out of standby mode.

73| With the IR remote in a functional position to activate the wireless module, place the animal in the behavior arena and begin the trial. Alternatively, for home-cage behavior, place the IR remote next to the cage and begin the trial.

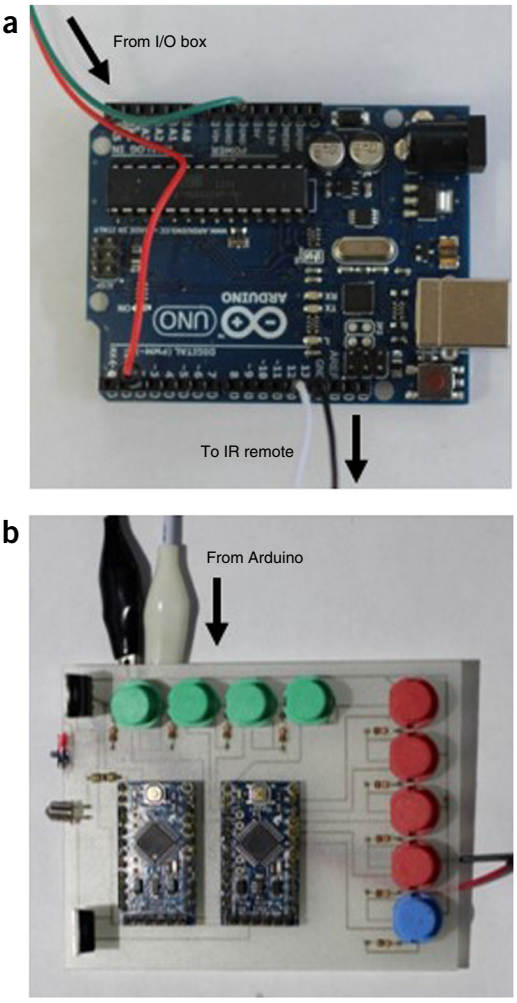

Figure 9 | Establishing automated control of the IR remote. (**a**) The jumper cables and alligator clips are properly connected to the pinouts of the Arduino UNO. (**b**) The alligator clips are attached to the pins representing the button for 1 Hz. The same approach can be used to take control of any pulse parameter button or heater button function.

74| Press the desired function buttons at the appropriate times for the experiment (e.g., press the button for Heater 1 to infuse the fluid in Chamber 1).
▲ **CRITICAL STEP** The experimental timing of fluid delivery will depend greatly on the nature of the delivered fluid. For example, viruses will probably require longer incubation periods than fast-acting pharmacological agents. Care should be taken to design experiments so that the time point of fluid delivery is congruent with the mechanism of action of the delivered fluid.

75| Visually confirm (in person or via video) that the proper indicator LEDs on the wireless control module are lit accordingly.
? TROUBLESHOOTING

76| After completion of the behavioral session, use the blue button on the IR remote to put all relevant optofluidic probes into power-saving mode.

77| Turn the power switch on the IR remote to the OFF position.

78| After the final behavioral session, if desired, sacrifice the animals and use the tissue for any manner of postmortem evaluation[21].
? TROUBLESHOOTING

? TROUBLESHOOTING
Troubleshooting advice can be found in **Table 1**.

TABLE 1 | Troubleshooting table.

Step	Problem	Possible reason	Possible solution(s)
11	Failure in detaching a glass substrate	Insufficient treatment with anti-stiction agent on the wafer mold	Increase the surface treatment time in Step 8
23	No electrical connection in heater metal traces	The surface of the FR-4 substrate is too rough or has scratches, which prevent uniform deposition of Cr/Au	Attach Kapton tape to the FR-4 substrate and make metal deposition on the Kapton film
28	FPC connector detaches while plugging in the wireless circuit cable	Loosely attached FPC connector	Apply 5 Minute Epoxy not only at both sides but also to the front of the connector to ensure tight bonding to the device substrate
38, 40, 78	Optofluidic probe is in the wrong area	Skull is improperly aligned in the stereotaxic frame	Follow the instructions provided for the stereotaxic equipment for ear bar placement and skull leveling. Species-specific ear bars may be required. If the suture lines for identifying bregma/lambda on the skull are difficult to visualize, a surgical microscope and/or treating the skull with hydrogen peroxide can be helpful
39	Dissolution of silk adhesive during sterilization	Too much exposure to ethanol	Most aqueous solutions will dissolve the silk adhesive. Do not soak the devices in ethanol, as this will promote dissolution of the adhesive. In our experience, rinsing the device with ethanol for ~15 s is sufficient to prevent widespread inflammation in mouse brain tissue[21]. Care should be taken to use appropriate sterilization techniques in higher mammals to avoid immune responses, such as EtO gas sterilization
43	Inability to remove the microneedle without movement	Blade used to cut the tape is too dull	Use a fresh scalpel blade for each surgery. It may be necessary to wait longer after penetration before removal of the microneedle
43,78	Optofluidic probe is in the wrong area	Too much movement during microneedle retraction	If removing the microneedle by hand, practice the technique or consider the use of the dual-arm stereotax as described. It may be necessary to wait longer after penetration before removal of the microneedle
60	Wireless module operation failure	Imperfect electrical connection between the wireless module and batteries	Use Kapton tape to tightly bond and fix electrodes of the wireless module and batteries. This is very important to avoid accidental disconnection of power by external shock during animal experiments
62	Optofluidic probe failure	Wireless control module cables to the connectors on the optofluidic device are misaligned	Carefully connect each cable, ensuring that it is in line with the connector. Slight misalignment can prevent proper powering of the heaters and/or μ-ILEDs. If using a device with μ-ILEDs, this connection can be tested at this point, before implantation
65	Inability to wirelessly trigger the device	Emission LED is too far from the subject	Position the remote closer to the behavioral assay and optimize device activation with a nonimplanted system
66	Inability to wirelessly trigger the device	Behavioral environment is not conducive to IR scattering or the angle of signal approach is improper	Consider the use of multiple, externally controlled and synchronized IR remotes
75	Premature battery failure	Spurious device powering from other light sources	Avoid direct exposure to sunlight or other high-intensity light sources. If exposure is necessary, use the remote to ensure that the device is on standby after exposure
75	Failure to expel fluids or power the μ-ILED	Imperfect electrical connection between the wireless module and heaters or μ-ILEDs	Ensure that the leads are straight and properly secured in the clasping connector

● TIMING

Step 1, preparation of flexible μ-ILED probes: 7 d

Steps 2–37 and 59–63, fabrication of flexible microfluidic probe, integration with μ-ILED probe, fabrication of thermally actuated pump, fluid loading and final assembly, preparation of IR wireless control module, preparation of device case, and device integration: 8 d

Steps 38–58, 64–78, implantation of optofluidic probe into targeted brain structure, preparation for behavioral testing, preparation of the behavioral assay for wireless control, and performing behavior testing: 2–14 d

Box 1, providing of external control of the IR remote: 1 h

ANTICIPATED RESULTS

By completing this protocol, the experimenter can expect to successfully fabricate ultrathin, flexible optofluidic neural probe systems with wireless fluid delivery and photostimulation capabilities. These probes are compatible with chronic implantation in freely moving animals and with most behavioral neuroscience experiments. The technology is well suited for either rats or mice (**Fig. 10a–c**) and reduces tissue damage as compared with other options for tethered drug delivery based on metal cannulas and tethered fiber optics for photostimulation[36]. The ultrathin, soft neural probe system overcomes these limitations by providing minimal invasiveness[78], biomechanical compatibility, high spatiotemporal control of both drug delivery and photostimulation, and wireless control. This multifunctional wireless system opens up new opportunities for advanced *in vivo* pharmacology and optogenetics behavior experiments[36]. Furthermore, the technology represents a step toward semiautomated *in vivo* experimentation. With fully self-contained features allowing for complete hands-free operation, behavioral experiments can be conducted without the researcher needing to have contact with the animal following implantation (after Step 63). Delivery of up to four different fluids is possible, and we have shown utility in viral gene transfer, local pharmacology, and paired optogenetic and pharmacological manipulation[36]. Depending on the resources of the laboratory and the demands of the experiment, it is possible that a single wireless control module can provide power to countless optofluidic neural probes, one at a time. The detailed fabrication process and technical procedures described in this protocol will benefit the wider community of neuroscientists with a neural device for minimally invasive spatiotemporal manipulation of neural circuits in awake, freely behaving animals with wireless drug delivery and photostimulation.

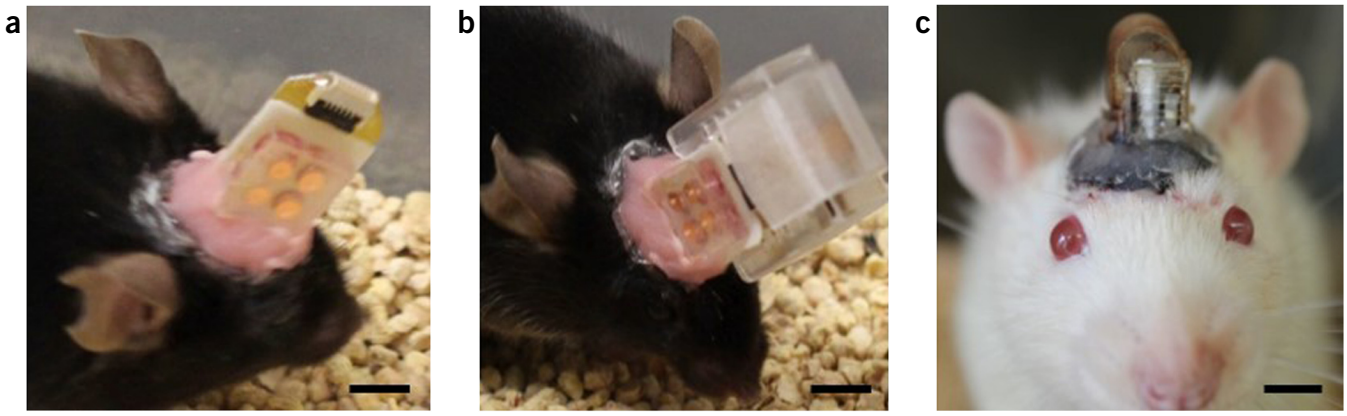

Figure 10 | Expected results following optofluidic neural probe implantation. (**a**) A mouse with an implanted optofluidic neural probe. (**b**) The same mouse prepared for wireless powering using the wireless control module. (**c**) A rat with a chronically implanted, completely self-contained wireless control module. Scale bars, 5 mm. All procedures were approved by the Animal Care and Use Committee of Washington University and conformed to US National Institutes of Health guidelines. Scale bars, 5 mm.

Note: Any Supplementary Information and Source Data files are available in the online version of the paper.

ACKNOWLEDGMENTS This work is supported by the EUREKA National Institute on Drug Abuse (NIDA) grant R01DA037152 (to M.R.B.), National Institute of Mental Health grant F31 MH101956 (to J.G.M.), and NIDA grant K99DA038725 (to R.A.). We thank the Bruchas laboratory and the laboratory of R.W. Gereau IV for helpful discussions and support. We thank W.Z. Ray for supporting the facilities for the rat surgery. All biomedical aspects of the device work were supported by a National Security Science and Engineering Faculty Fellowship of Energy (to J.A.R.) and startup funding from the University of Colorado Boulder (to J.-W.J.). The LED development was enabled by funding from the US Department of Energy, Division of Materials Sciences, under award no. DE-FG02-07ER46471 (to J.A.R.), the National Institutes of Health Common Fund National Institute of Neurological Disorders and Stroke grant R01NS081707 (to J.A.R. and M.R.B.), and the Materials Research Laboratory and Center for Microanalysis of Materials (grant DE-FG02-07ER46453 to J.A.R.).

AUTHOR CONTRIBUTIONS J.G.M., R.Q., G.S., S.L., M.H.I., K.-I.J., Y.L., R.A., and J.-W.J. performed the experiments. J.G.M., M.R.B., J.-W.J., and J.A.R. developed the protocol. J.G.M., M.R.B., J.-W.J., and J.A.R. wrote the manuscript.

COMPETING FINANCIAL INTERESTS The authors declare competing financial interests: details are available in the online version of the paper.

1. Rajasethupathy, P., Ferenczi, E. & Deisseroth, K. Targeting neural circuits. *Cell* **165**, 524–534 (2016).
2. Adamantidis, A.R., Zhang, F., Aravanis, A.M., Deisseroth, K. & de Lecea, L. Neural substrates of awakening probed with optogenetic control of hypocretin neurons. *Nature* **450**, 420–424 (2007).
3. Arenkiel, B.R. *et al. In vivo* light-induced activation of neural circuitry in transgenic mice expressing channelrhodopsin-2. *Neuron* **54**, 205–218 (2007).
4. Armbruster, B.N., Li, X., Pausch, M.H., Herlitze, S. & Roth, B.L. Evolving the lock to fit the key to create a family of G protein-coupled receptors potently activated by an inert ligand. *Proc. Natl. Acad. Sci. USA* **104**, 5163–5168 (2007).
5. Banghart, M., Borges, K., Isacoff, E., Trauner, D. & Kramer, R.H. Light-activated ion channels for remote control of neuronal firing. *Nat. Neurosci.* **7**, 1381–1386 (2004).
6. Güler, A.D. *et al.* Transient activation of specific neurons in mice by selective expression of the capsaicin receptor. *Nat. Commun.* **3**, 746 (2012).
7. Lima, S.Q. & Miesenböck, G. Remote control of behavior through genetically targeted photostimulation of neurons. *Cell* **121**, 141–152 (2005).
8. Zemelman, B.V., Lee, G.A., Ng, M. & Miesenböck, G. Selective photostimulation of genetically chARGed neurons. *Neuron* **33**, 15–22 (2002).
9. Zemelman, B.V., Nesnas, N., Lee, G.A. & Miesenbock, G. Photochemical gating of heterologous ion channels: remote control over genetically designated populations of neurons. *Proc. Natl. Acad. Sci. USA* **100**, 1352–1357 (2003).
10. Siuda, E.R. *et al.* Spatiotemporal control of opioid signaling and behavior. *Neuron* **86**, 923–935 (2015).
11. Yizhar, O., Fenno, L.E., Davidson, T.J., Mogri, M. & Deisseroth, K. Optogenetics in neural systems. *Neuron* **71**, 9–34 (2011).
12. Konermann, S. *et al.* Optical control of mammalian endogenous transcription and epigenetic states. *Nature* **500**, 472–476 (2013).
13. Schindler, S.E. *et al.* Photo-activatable Cre recombinase regulates gene expression *in vivo*. *Sci. Rep.* **5**, 13627 (2015).
14. Zhang, F. *et al.* Optogenetic interrogation of neural circuits: technology for probing mammalian brain structures. *Nat. Protoc.* **5**, 439–456 (2010).
15. Cardin, J.A. *et al.* Targeted optogenetic stimulation and recording of neurons *in vivo* using cell-type-specific expression of Channelrhodopsin-2. *Nat. Protoc.* **5**, 247–254 (2010).
16. Sparta, D.R. *et al.* Construction of implantable optical fibers for long-term optogenetic manipulation of neural circuits. *Nat. Protoc.* **7**, 12–23 (2011).
17. Sternson, S.M. & Roth, B.L. Chemogenetic tools to interrogate brain functions. *Annu. Rev. Neurosci.* **37**, 387–407 (2014).
18. Tye, K.M. & Deisseroth, K. Optogenetic investigation of neural circuits underlying brain disease in animal models. *Nat. Rev. Neurosci.* **13**, 251–266 (2012).
19. Zorzos, A.N., Boyden, E.S. & Fonstad, C.G. Multiwaveguide implantable probe for light delivery to sets of distributed brain targets. *Opt. Lett.* **35**, 4133–4135 (2010).
20. Zorzos, A.N., Scholvin, J., Boyden, E.S. & Fonstad, C.G. Three-dimensional multiwaveguide probe array for light delivery to distributed brain circuits. *Opt. Lett.* **37**, 4841–4843 (2012).
21. Kim, T. *et al.* Injectable, cellular-scale optoelectronics with applications for wireless optogenetics. *Science* **340**, 211–216 (2013).
22. Al-Hasani, R. *et al.* Distinct subpopulations of nucleus accumbens dynorphin neurons drive aversion and reward. *Neuron* **87**, 1063–1077 (2015).
23. Wu, F. *et al.* Monolithically integrated μLEDs on silicon neural probes for high-resolution optogenetic studies in behaving animals. *Neuron* **88**, 1136–1148 (2015).
24. McAlinden, N., Gu, E., Dawson, M.D., Sakata, S. & Mathieson, K. Optogenetic activation of neocortical neurons *in vivo* with a sapphire-based micro-scale LED probe. *Front. Neural Circuits* **9**, 25 (2015).
25. Stachniak, T.J., Ghosh, A. & Sternson, S.M. Chemogenetic synaptic silencing of neural circuits localizes a hypothalamus→midbrain pathway for feeding behavior. *Neuron* **82**, 797–808 (2014).
26. Park, S.I. *et al.* Ultraminiaturized photovoltaic and radio frequency powered optoelectronic systems for wireless optogenetics. *J. Neural Eng.* **12**, 056002 (2015).
27. Montgomery, K.L. *et al.* Wirelessly powered, fully internal optogenetics for brain, spinal and peripheral circuits in mice. *Nat. Methods* **12**, 969–974 (2015).
28. Park, S.I. *et al.* Soft, stretchable, fully implantable miniaturized optoelectronic systems for wireless optogenetics. *Nat. Biotechnol.* **33**, 1280–1286 (2015).
29. Ameli, R., Mirbozorgi, A., Neron, J.-L., LeChasseur, Y. & Gosselin, B. A wireless and batteryless neural headstage with optical stimulation and electrophysiological recording. in *2013 35th Annual International Conference of the IEEE Engineering in Medicine and Biology Society (EMBC)* 5662–5665 (2013).
30. Lee, S.T. *et al.* A miniature, fiber-coupled, wireless, deep-brain optogenetic stimulator. *IEEE Trans. Neural Syst. Rehabil. Eng.* **23**, 655–664 (2015).
31. Rossi, M.A. *et al.* A wirelessly controlled implantable LED system for deep brain optogenetic stimulation. *Front. Integr. Neurosci.* **9**, 8 (2015).
32. Iwai, Y., Honda, S., Ozeki, H., Hashimoto, M. & Hirase, H. A simple head-mountable LED device for chronic stimulation of optogenetic molecules in freely moving mice. *Neurosci. Res.* **70**, 124–127 (2011).
33. Wentz, C.T. *et al.* A wirelessly powered and controlled device for optical neural control of freely-behaving animals. *J. Neural Eng.* **8**, 046021 (2011).
34. Siuda, E.R. *et al.* Optodynamic simulation of β-adrenergic receptor signalling. *Nat. Commun.* **6**, 8480 (2015).
35. McCall, J.G. *et al.* Fabrication and application of flexible, multimodal light-emitting devices for wireless optogenetics. *Nat. Protoc.* **8**, 2413–2428 (2013).
36. Jeong, J.-W. *et al.* Wireless optofluidic systems for programmable *in vivo* pharmacology and optogenetics. *Cell* **162**, 662–674 (2015).
37. Parker, K.E., McCall, J.G. & Will, M.J. Basolateral amygdala opioids contribute to increased high-fat intake following intra-accumbens opioid administration, but not following 24-h food deprivation. *Pharmacol. Biochem. Behav.* **97**, 262–266 (2010).
38. Boschi, G., Launay, N. & Rips, R. Implantation of an intracerebral cannula in the mouse. *J. Pharmacol. Methods* **6**, 193–198 (1981).
39. Chefer, V.I., Thompson, A.C., Zapata, A. & Shippenberg, T.S. Overview of brain microdialysis. *Curr. Protoc. Neurosci.* Unit 7.1, supplement 47 (2009).
40. Ruigrok, T.J.H. & Apps, R. A light microscope-based double retrograde tracer strategy to chart central neuronal connections. *Nat. Protoc.* **2**, 1869–1878 (2007).
41. Conte, W.L., Kamishina, H. & Reep, R.L. Multiple neuroanatomical tract-tracing using fluorescent Alexa Fluor conjugates of cholera toxin subunit B in rats. *Nat. Protoc.* **4**, 1157–1166 (2009).
42. Spieth, S. *et al.* An intra-cerebral drug delivery system for freely moving animals. *Biomed. Microdevices* **14**, 799–809 (2012).
43. Canales, A. *et al.* Multifunctional fibers for simultaneous optical, electrical and chemical interrogation of neural circuits *in vivo*. *Nat. Biotechnol.* **33**, 277–284 (2015).
44. Farra, R. *et al.* First-in-human testing of a wirelessly controlled drug delivery microchip. *Sci. Transl. Med.* **4**, 122ra21–122ra21 (2012).
45. Hoare, T. *et al.* A magnetically triggered composite membrane for on-demand drug delivery. *Nano Lett.* **9**, 3651–3657 (2009).
46. Hoare, T. *et al.* Magnetically triggered nanocomposite membranes: a versatile platform for triggered drug release. *Nano Lett.* **11**, 1395–1400 (2011).
47. Timko, B.P. *et al.* Near-infrared-actuated devices for remotely controlled drug delivery. *Proc. Natl. Acad. Sci. USA* **111**, 1349–1354 (2014).
48. Minev, I.R. *et al.* Biomaterials. Electronic dura mater for long-term multimodal neural interfaces. *Science* **347**, 159–163 (2015).
49. Richards, N. & McMahon, S.B. Targeting novel peripheral mediators for the treatment of chronic pain. *Br. J. Anaesth.* **111**, 46–51 (2013).
50. Scheib, J. & Höke, A. Advances in peripheral nerve regeneration. *Nat. Rev. Neurol.* **9**, 668–676 (2013).
51. Banghart, M.R. & Sabatini, B.L. Photoactivatable neuropeptides for spatiotemporally precise delivery of opioids in neural tissue. *Neuron* **73**, 249–259 (2012).
52. Kramer, R.H., Mourot, A. & Adesnik, H. Optogenetic pharmacology for control of native neuronal signaling proteins. *Nat. Neurosci.* **16**, 816–823 (2013).
53. Tochitsky, I. *et al.* Restoring visual function to blind mice with a photoswitch that exploits electrophysiological remodeling of retinal ganglion cells. *Neuron* **81**, 800–813 (2014).
54. Polosukhina, A. *et al.* Photochemical restoration of visual responses in blind mice. *Neuron* **75**, 271–282 (2012).
55. Myers, M.W., Laughlin, C.A., Jay, F.T. & Carter, B.J. Adenovirus helper function for growth of adeno-associated virus: effect of temperature-sensitive mutations in adenovirus early gene region 2. *J. Virol.* **35**, 65–75 (1980).

56. Sinn, P.L., Sauter, S.L. & McCray, P.B. Gene therapy progress and prospects: development of improved lentiviral and retroviral vectors – design, biosafety, and production. *Gene Ther.* **12**, 1089–1098 (2005).
57. Beer, C., Meyer, A., Müller, K. & Wirth, M. The temperature stability of mouse retroviruses depends on the cholesterol levels of viral lipid shell and cellular plasma membrane. *Virology* **308**, 137–146 (2003).
58. Kawai, A. & Takeuchi, K. Temperature-sensitivity of the replication of rabies virus (HEP-flury strain) in BHK-21 cells I. Alteration of viral RNA synthesis at the elevated temperature. *Virology* **186**, 524–532 (1992).
59. Croughan, W.S. & Behbehani, A.M. Comparative study of inactivation of herpes simplex virus types 1 and 2 by commonly used antiseptic agents. *J. Clin. Microbiol.* **26**, 213–215 (1988).
60. Petr, G. & Jiran, E. The effect of temperature on the hemagglutinin activity of the canine adenovirus (infectious canine hepatitis virus). *Zentralbl Veterinärmed B* **17**, 569–581 (1970).
61. Merten, O.-W., Gény-Fiamma, C. & Douar, A.M. Current issues in adeno-associated viral vector production. *Gene Ther.* **12**, S51–S61 (2005).
62. Resendez, S.L. *et al.* Visualization of cortical, subcortical and deep brain neural circuit dynamics during naturalistic mammalian behavior with head-mounted microscopes and chronically implanted lenses. *Nat. Protoc.* **11**, 566–597 (2016).
63. Cetin, A., Komai, S., Eliava, M., Seeburg, P.H. & Osten, P. Stereotaxic gene delivery in the rodent brain. *Nat. Protoc.* **1**, 3166–3173 (2007).
64. Cui, G. *et al.* Deep brain optical measurements of cell type-specific neural activity in behaving mice. *Nat. Protoc.* **9**, 1213–1228 (2014).
65. Carlezon, W.A. & Chartoff, E.H. Intracranial self-stimulation (ICSS) in rodents to study the neurobiology of motivation. *Nat. Protoc.* **2**, 2987–2995 (2007).
66. Kim, D.-H. *et al.* Dissolvable films of silk fibroin for ultrathin conformal bio-integrated electronics. *Nat. Mater.* **9**, 511–517 (2010).
67. Tao, H. *et al.* Silk-based conformal, adhesive, edible food sensors. *Adv. Mater.* **24**, 1067–1072 (2012).
68. Hwang, S.-W. *et al.* A physically transient form of silicon electronics. *Science* **337**, 1640–1644 (2012).
69. Artificial cerebrospinal fluid (ACSF). *Cold Spring Harb. Protoc.* http://cshprotocols.cshlp.org/content/2011/9/pdb.rec065730.full?text_only=true (2011).
70. Ting, J., Daigle, T., Chen, Q. & Feng, G. in *Patch-Clamp Methods and Protocols* (eds. Martina, M. & Taverna, S.) 221–242 (New York: Springer, 2014).
71. Jeong, J.W. *et al.* Soft microfluidic neural probes for wireless drug delivery in freely behaving mice. in *2015 Transducers—2015 18th International Conference on Solid-State Sensors, Actuators and Microsystems (TRANSDUCERS)* 2264–2267 (2015).
72. Walf, A.A. & Frye, C.A. The use of the elevated plus maze as an assay of anxiety-related behavior in rodents. *Nat. Protoc.* **2**, 322–328 (2007).
73. Noldus, L.P., Spink, A.J. & Tegelenbosch, R.A. EthoVision: a versatile video tracking system for automation of behavioral experiments. *Behav. Res. Methods Instrum. Comput.* **33**, 398–414 (2001).
74. de Chaumont, F. *et al.* Computerized video analysis of social interactions in mice. *Nat. Methods* **9**, 410–417 (2012).
75. McCall, J.G. *et al.* CRH engagement of the locus coeruleus noradrenergic system mediates stress-induced anxiety. *Neuron* **87**, 605–620 (2015).
76. Deacon, R.M.J. & Rawlins, J.N.P. T-maze alternation in the rodent. *Nat. Protoc.* **1**, 7–12 (2006).
77. Cunningham, C.L., Gremel, C.M. & Groblewski, P.A. Drug-induced conditioned place preference and aversion in mice. *Nat. Protoc.* **1**, 1662–1670 (2006).
78. Jeong, J.-W. *et al.* Soft materials in neuroengineering for hard problems in neuroscience. *Neuron* **86**, 175–186 (2015).